<u>**Response to Comments of Referee #1**</u>

We thank the reviewer for his/her carefully reading of the manuscript and providing very constructive criticism.

Specific comments
<u>**P 1484, l 24:**</u> The introduction refers mainly to extreme wind speeds, which I understand as the maximum wind speed within a certain period. However, you use daily mean winds. I would like to see the statistical relation between daily means and daily extremes as the maximum daily gust.

Yes, we understand the reviewer's definition of extreme. Nevertheless, we see 'extreme' as a matter of definition. It would also be possible to define extreme referring to monthly means e.g. Schönwiese et al. (2003) or even seasonal or annual means. As far as we know there is no widely excepted definition of extreme wind. Extreme events, in general, are events that occur scarcely. The precise definition will depend on the particular application. For instance, for applications to aeolian or insurance sectors, extreme gusts of 10 minutes will be relevant for the safety of the rotors or houses. For more metereological/climatological applications, daily means could be more relevant, for instance for storm surges. Here, we choose to use the 95th and 99th percentile of daily wind speed because this ensures that only 'rare' wind speeds are used. While the analysis of wind gusts will be interesting in itself, unfortunately we are not able to follow the reviewer's wish to see 'the statistical relation between daily means and daily extremes as the maximum daily gust.' because this values are not available for most of the simulations. For instance, although the time steps of the regional models analysed here would be enough to resolve wind gusts, the data are usually stored as hourly means

We tried to make sure that our definition of extreme wind was expressed more clearly by:

<u>New version:</u> *The analysis of several percentiles and their differences allows the determination of basic changes in the characteristics of wind speed distributions, hence it is possible to investigate if it shifts with time with unchanged shape and/or whether its width changes. Thus, we can discriminate between a change in the mean and/or in the extreme of the wind speed distribution. In our case 'extreme' means the tail of the distribution, which includes values above the 95th percentile. For instance, increasing diffM and diffE values would show a broadening of the distribution which means higher extreme wind speeds.*

<u>Old version:</u> *The analysis of several percentiles and their differences allows the determination of basic changes in the characteristics of wind speed distributions, hence it is possible to investigate if it shifts with time with unchanged shape and/or whether its width changes.*

<u>**P 1486, l 11:**</u> The description of the MPI-ESM lacks the description of the ocean component.

This is true. However, this is described in detail in other publications which we refer to. We choose to not explicitly explain the ocean component because it only plays a minor role for our focus.

<u>**P 1487, l 26:**</u> What do you mean with "the same nudging technique"? Do you mean it is the same as in NCEP/NCAR?

The reviewer is right, this is confusing. We removed this part. The sentence now reads as follows:

<u>New version:</u> I*n addition we analyse the high resolution regional product coastDat2 (Geyer, 2014) resulting from a simulation with the regional model CCLM and driven by the global NCEP/NCAR reanalysis using a spectral nudging technique (after von Storch et al. (2000)).*

<u>Old version:</u> *In addition we analyse the high resolution regional product coastDat2 (Geyer, 2014) resulting from a simulation with the regional model CCLM and driven by the global NCEP/NCAR reanalysis using also the same spectral nudging technique (after von Storch et al., 2000).*

P 1488, l 1: How large are the model domains of both RCMs? Perhaps, an overview map would be nice to illustrate the model domains and the study area.

We have now included a figure demonstrating the RCM domains. In accordance with other comments this is a combined figure showing the RCM domains as well as the land-see-masks of all data sets.

P 1488, l 17: You average over the entire selected area as far as I understand. I am a bit concerned about the impact of the ocean and the corresponding land-sea-mask (see comments below). How would your results look like if you distinguish between land and ocean points?

The table includes the spatially averaged data as a summary of the correlation analysis but the subsequent figures and the corresponding discussions do show the spatial correlation maps, including the land and ocean areas. It seems to us that these figures include the information requested by the reviewer.

P 1488, l 18: The explanation of the computation of the temperature gradient (P 1489, l 1-3) should be moved to the end of this sentence. Moreover, why do you use absolute values for the gradient? You cannot exclude situations when the temperature gradient is reversed and that will be hidden by the use of absolute values. In addition, what is the impact of the ocean for tGrad? About one third of the northern boundary is located over the North Atlantic which is characterized by positive temperature anomalies compared with the rest of the domain during winter.

We moved the whole paragraph as mentioned the following way:
The three climate parameters analysed regarding their influence on wind speed are (1) mean seasonal near-surface air temperature (mTemp), (2) mean seasonal meridional temperature gradient (tGrad) and (3) the North Atlantic Oscillation index (NAO).
The temperature gradient is calculated as the absolute value of the difference between the northern (N) and the southern (S) half of the investigation area tGrad = abs(N −S) for each model simulation. Due to the different resolutions the exact geographical domains of N and S differ. Therefore the border between both varies from around 53°N to 57°N.
The North Atlantic Oscillation (NAO) index is defined as the leading pattern resulting from principal component analysis (PCA) of the winter mean sea-level pressure (MSLP) field. This dominant pattern of variability is characterized by a low pressure system over Iceland and a high pressure system over the Azores (exemplary shown for ECHAM6 in Fig. 2). As MSLP field we used the GCM gridded pressure information of the North Atlantic and European area. This domain approximately spans from 70± W to 30± E longitude (from ~ Boston to Istanbul) and from 70± N to 20± N latitude (from ~ Tromsø to the southern part of Morocco). For computations conducted for the RCM simulations we used the NAO patterns derived from these GCM fields as well.

For the computation of the meridional gradient we are using either 30-year means for the long simulations or 5-year means for the shorter reanalysis data. Situations when the temperature gradient is

reversed (N>S) do not occur for these computations.

Concerning the ocean, the reviewer is right that the ocean has an impact on the temperature gradient, some others e.g. the atmospheric circulation or sea ice also do have an influence. However, we are analysing the influence that the large-scale temperature gradient may have on the occurrence of extremes. One of the reasons is that, under anthropogenic greenhouse gas forcing, the large-scale gradient is projected to decrease, so that overall the baroclinicity of the atmosphere would also tend to decrease, possibly influencing the extreme events. Although the individual influence of the ocean, or ice-cover etc., may be interesting in itself, the analysis of these relationships is beyond the scope of our study.

 P 1488, l 20: How are the results affected by the running mean computations? How strong are the statistical relations for yearly values?

We choose to use running mean values because the internal variability of daily wind is very high. This means that during one year the wind speed distribution can be very broad although the temperature is not different to another year. The focus of our analyses lies on understanding the long-term changes that may be brought about by multi-decadal climate change. Therefore using yearly values would lead to very small correlations between wind speed distribution and mean temperature. We hope to circumvent this effect by including more values than only 90 days per winter through combining 30/5 winter seasons.

P 1489, l 4: It is not clear to me how you compute the NAOI. I guess you do not use the global fields from the GCMs, or? How did you compute the NAOI for the RCMs where the model domain might not even cover the Azores?

We agree with this criticism and tried to explain our method more clearly.
New version: *The North Atlantic Oscillation (NAO) index is defined as the leading pattern resulting from principal component analysis (PCA) of the winter mean sea-level pressure (MSLP) field. This dominant pattern of variability is characterized by a low pressure system over Iceland and a high pressure system over the Azores (exemplary shown for ECHAM6 in Fig. 2). As MSLP field we used the GCM gridded pressure information of the North Atlantic and European area. This domain approximately spans from 70± W to 30± E longitude (from ~ Boston to Istanbul) and from 70± N to 20± N latitude (from ~ Tromsø to the southern part of Morocco). For computations conducted for the RCM simulations we used the NAO patterns derived from these GCM fields as well.*

Old version*: The North Atlantic Oscillation (NAO) index is defined as the leading pattern resulting from principal component analysis (PCA) of the winter mean sea-level pressure (MSLP) field. This dominant pattern of variability is characterized in all simulations by a low pressure system over Iceland and a high pressure system over the Azores.*

P 1491, l 6: Figure 1c) clearly indicates that the correlation is opposite over land and the ocean. Therefore I wonder about the prescribed ocean temperatures. I guess they are taken from ECHO-G. Consequently, you might see a similar response over the ocean. More general, it might be interesting to see the correlations of table 2 split into ocean and land points. By doing that, you would also get correlations that are almost independent of the forest cover – namely the ones over the ocean.

Yes, the MM5 ocean temperatures are taken from its driving simulation ECHO-G. However, a similar

response over the ocean is only visible for the P50 correlation. For the STD correlation with mTemp MM5 also shows negative values over sea.

Table 2 includes the spatially averaged data as a summary of the correlation analysis but the subsequent figures and the corresponding discussions do show the spatial correlation maps, including the land and ocean areas. It seems to us that these figures include the information requested by the reviewer. Moreover, only two simulations (ECHAM5, ECHAM6) are affected by the time dependent vegetation forcing. But this is precisely why we also included an analysis of two time slices. The period prior the deforestation enabled us to analyse the link between temperature and wind independently from the land-use change forcing, thus we can compare these two model setups with the other data sets. Nevertheless, it has to be borne in mind that the common long-term trend caused by deforestation may explain only part of the total correlation. The interannual and interdecadal variability will also affect the value of the correlation, and at these time scales the changes in land-use should not have an influence, since its rate of change is much slower.

P 1491, l 15+19: Shouldn't it be P95 and P99?

Yes, we changed this.

P 1493, l 16: The last two lines of table 2 do not show the relationship of the NAO and the mean temperature. I think table 2 is not complete, e.g. NAO-P95 is missing.

We extended Table 2.

P 1495, l 3: P99-P50 is not shown in table 2. However, there is diffM (P95-P50) which supports the statement.

We did not include P99-P50 because the question whether the wind speed distribution expands can also be answered with diffM (P95-P50), as the reviewer already mentioned.

P 1495, l 6: What is the impact of the land-sea-mask for the GCM results? I think the Baltic Sea and especially the connection to the North Sea must lead to a very odd land-sea-mask since the ocean cells are very large. Perhaps, the agreement between the GCMs and the RCMs would be larger if you consider the land-sea-masks. In any case, I would like to see the land-sea-masks of all considered simulations.

P 1496, l 5: As stated before, different land-sea-masks in the different set-ups might play a crucial role.

P 1496, l 20: The "different spatial fingerprint" might be caused by different coastlines.

We assume these three points concern the same issue, hence we give a summarized answer: We have the impression that we did not communicate our analysis method properly. We did not calculate correlations between each grid point of the wind speed distribution parameters (e.g. STD) and each grid point of the atmospheric drivers (mTemp, tGrad, NAO) but used the spatial mean of the latter, averaged over the whole domain. This is done due to the scope of our analysis to investigate the large-scale influences on the wind speed distribution.

However, we include a figure which demonstrates the land-sea-masks of all considered data sets.

P 1495, l 16: Do you refer to Table 2?

We now refer to Table 2:

New version: *Therefore, we also analysed the relationship between the parameters of the wind speed distribution and tGrad (Table 3).*

Old version: *Therefore, we also analysed the relationship between the parameters of the wind speed distribution and tGrad.*

P 1495, l 20: You do not show results for P99-P50. Therefore, I am not sure whether you refer to table 2 or one of your figures.

We apologise for this typing error as it should be P99-P95 (diffE), which is included in Table 3.

P 1498, l 20: The value is not bold in the table. So, is it significant?

No, the reviewer is right, this is not a statistical significant value. However, values without statistical significance still allow for some conclusions on relationships if they show a consistent pattern across several data sets..

P 1499, l 14: Information from Fig. 5 is not really used. Two out of the three time series can be found in Fig. 6 as well. Since a more detailed comparison between the curves of Fig. 5 is not done, you might skip this figure.

We agree with this point and excluded the Figure.

P 1499, l 16: I see an increase of both parameters over the last 250 years, at least. And that corresponds to a period of constant temperature rise in the ECHO-G simulation.

We do not see an increase of the STD over the last 250 years for ECHO-G but maybe over the last 100 years. Nevertheless, the mean temperature is rising since the beginning of the 17th century. For ECHAM6 both time series start to rise at approximately the same time.

P 1500, l 15: Yes, it seems that the land-use changes have the main impact. That makes large parts of the manuscript irrelevant. There must be control simulations available (some without any variation in the forcing). It seems they would serve much better for your investigations. Why did you use transient simulations?

This is a fair point. Indeed for the second half of the simulation with prescribed land-use variability the correlation between the wind distribution and temperature could be modulated by the long-term effect of land-use change, since both have a long-term centennial trend. But this is precisely why we also included an analysis of two time slices. The period prior the deforestation enabled us to analyse the link between temperature and wind independently from the land-use change forcing, thus we can compare these two model setups with the other data sets. Nevertheless, it has to be borne in mind that the common long-term trend may explain only part of the total correlation. The interannual and interdecadal variability will also affect the value of the correlation, and at these time scales the changes in land-use should not have an influence, since its rate of change is much slower.

We use the transient simulations as the included deforestation is supposed to represent the actual land-use change, and therefore these two simulations consider an important aspect which influences the link between temperature, NAO and the wind speed distribution. This allows for the identification of the

additional aspect of deforestation. Note that one of the goals of our analysis is to answer the question of whether large-scale temperature affects the distribution of surface winds. In the past and in the future, temperature is affected by transient forcings, and thus transient simulations should yield a more realistic answer. For instance, an analysis of a control simulation with constant forcing would have identified correlations between the wind distribution and variations in the temperature gradient which might bear little relevance for temperature changes caused by the external forcing. In addition, the analysis of proxy records representing past conditions will be affected by all forcings. Our analysis has, for instance, identified that deforestation can be an important factor for the wind distribution, which can be important when interpreting natural proxies based on lake sediments or coastal dunes.

Note that we extended this section by analysing the deforestation in more detail.

P 1501, l 8: "The study is based on correlations..." But, large parts of the correlations seem to controlled by deforestation. Me feeling is that it is hard to draw any conclusion from table 2, which is the main object of this manuscript.

Please note, that only two simulations (ECHAM5 and ECHAM6) include time-depended vegetation. As mentioned above we argue that our analysis allow for the investigation of temperature and NAO relationships to wind speed distribution due to the analysis of time slices, with and without deforestation.

P 1503, l 14: An extreme refers in your manuscript to daily means. Most people might think in terms of maximum gusts. That should be clarified.

As far as we know there is no widely excepted definition of extreme wind. However, we tried to explain our definition more clearly by:

New version: *The analysis of several percentiles and their differences allows the determination of basic changes in the characteristics of wind speed distributions, hence it is possible to investigate if it shifts with time with unchanged shape and/or whether its width changes. Thus, we can discriminate between a change in the mean and/or in the extreme of the wind speed distribution. In our case 'extreme' means the tail of the distribution, which includes values above the 95th percentile. For instance, increasing diffM and diffE values would show a broadening of the distribution which means higher extreme wind speeds.*

Old version: *The analysis of several percentiles and their differences allows the determination of basic changes in the characteristics of wind speed distributions, hence it is possible to investigate if it shifts with time with unchanged shape and/or whether its width changes.*

Section 5: I miss the relation to previous work. I count only two references for the entire section "Discussion and conclusions". You should at least compare to the studies mentioned in your introduction, e.g. Fischer-Bruns et al. (2005). Clearly, I see the need to discuss the role of the ocean (prescribed or modelled) as well as the land-sea-mask.

We extended the "Discussion and conclusions" by brief discussions of our results compared to Rutgersson et a. (2015), Li and Woollings (2014), Fischer-Bruns et al. (2005) and Hall (2014).

Table 2: Something seems to be missing in the table. What about NAO-P95, NAO-P99, NAO-diffM, NAO-diffE? Moreover, you mentioned in the text the relationship of NAO-mTemp and NAO-

tGrad, which are not shown in the table.

We extended Table 2.

Figures 1-4 are rather small. It might be possible to rearrange them so that every single figure becomes larger. You could try to order them as: upper: three GCMs middle: two RCMs lower: two reanalysis

We enlarged the Figures and their labels and hope they read now better.

Caption of figure 7: The abbreviations P1 and P2 as defined in this caption are not used in the text. Moreover, it becomes confusing with the abbreviations introduced in the text (P 1500, l 22).

We included the abbreviations P1 and P2 in the text and changed the abbreviations on page 1500, line 22 to TP1 and TP2.
New version: *The difference in tree fraction in each model grid-cell between the periods 1871-1990 AD (P1) and 1001-1091 AD (P2) is shown in Figure 10b.*

Old version: *The difference in tree fraction in each model grid-cell 5 between the periods 1871–1990 AD and 1001–1091AD is shown in Fig. 7b.*

New version: *Therefore, this statistical effect can be disentangled by separating the analysis of these simulations into two time periods (TP1: years 850-1500 AD, TP2: years 1500-2005 AD). The correlations between mean temperature and the width of the wind distribution does show a difference in the correlation. For TP1 of ECHAM6 mTemp-diffM is around 0 and mTemp-diffE -0.25, for P2 0.63 and 0.57, respectively. For TP1 of ECHAM5 mTemp-diffM is -0.26 and mTemp-diffE is -0.38, for TP2 0.26 and 0.12, respectively. Both time periods in the GCMs show different signs for the relation between mean temperature and the shape of the wind speed distribution.*

Old version: *This statistical effect can be disentangled by separating the analysis of these simulations into two parts (P1: years 850-1500AD, P2: years 1500-2005 AD). The correlations between mean temperature and the width of the wind distribution does show a difference in the correlation. For P1 of ECHAM6 mTemp-diffM is around 0 and mTemp-diffE -0.25, for P2 0.63 and 0.57, respectively. For P1 of ECHAM5 mTemp-diffM is -0.26 and mTemp-diffE is -0.38, for P2 0.26 and 0.12, respectively. Both parts in the GCMs show different signs for the relation between mean temperature and the shape of the wind speed distribution.*

Technical corrections
P 1496, l 23: The sentence sounds strange and needs to be rewritten. You might want to use a formulation like ECHAM6 is the latest version of the ECHAM series/family.

We choose to remove this sentence as it is a repetition of the Data-section.

P 1498, l 6: "mTemp and P50", please refer to Figure 1f+g) Moreover, move you reference to figure 2 from the of the sentence behind "STD field".

New version: *The spatially resolved correlation between mTemp and P50 (Fig. 3f+g) and the STD field (Fig. 4f+g) is also dominated by positive values, with highest coefficients over southern Norway, and weaker or slightly negative correlations in the southern regions of the domain.*

<u>Old version:</u> *The spatially resolved correlation between mTemp and P50 and the STD field is also dominated by positive values, with highest coefficients over southern Norway, and weaker or slightly negative correlations in the southern regions of the domain (s. Figure 2f).*

<u>Additional Information:</u> Please note that during the revision of the manuscript we realised that we had accidentally used a different ECHAM5 simulation than the one that had been in fact used to drive the model CCLM. We used the ECHAM5-E1 run, which differs from the actual CCLM driving version ECHAM5-E2 only in a weaker solar forcing. Our conclusions do not change.

References:
C.-D. Schönwiese, J. Grieser, S. Trömel (2003): Secular change of extreme monthly precipitation in Europe, *Theoretical and Applied Climatology,* Sep. 2003, Vol. 75, Issue 3-4, pp 245-250

Response to Comments of Referee #2

We thank the reviewer for his/her carefully reading of the manuscript and providing very constructive criticism.

Reviewer: First of all, I find the description of the simulations not precise enough. External forcing are key elements of simulations, and as its stands the manuscript does not offer any clear way to estimate the forcing present in the simulation. Indeed, the manuscript quite surprisingly ends by arguing that land-use forcing differences among the simulations may strongly affect the results presented. The same can hold for other external forcings. Since there is no figure presenting them, we cannot really estimate this. Moreover, even the land-use change is very rapidly depicted in Fig. 7 with comparison of only two periods from a millennium simulation. This is not enough to prove anything: time series are necessary as well.

We understand the criticism regarding the brief model description. The reason was that these simulations have been already analysed and described in great detail in their respective publication, and therefore we decided to be brief in the description, referring the reader to the original references. However, taking into account the reviewer's suggestion we extended this part and described the prescribed forcings in greater detail in an additional subsection.
Still, note that the illustration of the land-use changes as a single time series is difficult, because land-cover is characterized by several types of land-use (forest, pasture, bare soil, etc): In our case, it is the forest fraction that seems to be the most significant for wind, and we included a figure showing the time series of the forest fraction in comparison with the STD of wind speed for ECHAM6. Moreover, we extended the explanations in section 'Centennial-scale evolution of the wind speed variance over the past millennium'.

Reviewer: Secondly, and this may be related with my first point, I have an issue with the fact that all the statistics presented in the different figures are not provided for same time period, but only for available time period for each simulation. While I understand the authors cannot do very differently for short reanalysis, I think it is necessary to evaluate sensitivity of the results to the time period chosen to compute the correlations. Indeed, some time periods, like the recent one, can be strongly affected by diverse forcings, which may affect the robustness of any searched relationship. For instance, the change in land use, as stated by the authors in their final part, can strongly affect relation between temperature gradient and wind, while it is not temperature that causes the changes in wind but surface roughness. Hence, the authors should compare simulations on similar time period, and we need to know more clearly and quantitatively what are the variations of the forcings over this time period. For instance comparing 1655-1999 period for CCLM and 850-2005 period for ECHAM5 (his father) is not rigorous from my point of view.

We have now extended our analysis with a new subsection investigating the two overlapping time periods without reanalysis data (1655-1990) and with reanalysis data (1948-1990). We re-calculated the correlation values for Table 2 and re-plotted figures 1 to 4. A new subsection describes the differences between those time periods and two new figures show the results for 1948-1990 for mTemp-P50 and mTemp-STD.

Specific comments:
p. 1481, l. 6: I would add a "Indeed" before "Section 3" for logical clarity

We agree and added an "Indeed".

p. 1482, l. 1: Any reference to support the claim of the first sentence?

New Version: *It is thus very plausible that the NAO is also involved in the variations of the distribution of daily wind speeds, e.g. Wang et al. (2011) state that NAO variations show a relationship with the 99th percentile of wind speed.*

Old version: *It is thus very plausible that it is also involved in the variations of the distribution of daily wind speeds.*

p. 1482, l. 3: "change in temperature". Where?

New Version: *The NAO itself could also be related to changes in European near-surface winter temperature (Rutgersson et al., 2015).*

Old version: *The NAO itself could also be related to changes in temperature.*

p. 1482, l. 3-5: Paper by Cattiaux & Cassou (2013) shows that this is only true for SLP and less clear in altitude (Z500). Please discuss a little bit the results from Gillet and Fyfe (2013) in regard to Cattiaux & Cassou (2013).

New Version: *In this regard, scenario simulations indicate a contradicting tendency of the NAO in a warmer future, depending on whether it is defined from the sea-level pressure (SLP) gradient or from the geopotential height at 500 mbar (Z500). Gillett and Fyfe (2013) showed that the meridional SLP gradient will tend to become steeper polewards. On the other hand Cattiaux and Cassou (2013) also found a positive trend of the SLP gradient but found a negative trend of the Z500 gradient. Our study focuses on surface winds which are rather influenced by SLP variations. The link between the NAO and external climate forcing over the past centuries is, however, unclear in climate simulations (Gómez-Navarro and Zorita, 2013).*

Old version: *In this regard, scenario simulations in general indicate a tendency towards a stronger meridian pressure gradient in the future (Gillett and Fyfe, 2013), but the link between the NAO and external climate forcing over the past centuries is unclear in climate simulations (Gómez-Navarro and Zorita, 2013).*

p. 1482, l. 7: Please remind the reader for which region you say that.

New version: *Thus, for Northern Europe, from the dynamical point of view it is not clear how the distribution of wind speed would respond to changes in temperature.*

Old version: *Thus, from the dynamical point of view it is not clear how the distribution of wind speed would respond to changes in temperature.*

p. 1482, l. 8-11: I also assume that the time length of available observations is a bit short to satisfactorily assess changes in extremes, which occur scarcely.

New version: *The analysis of long-term trends in wind extremes and storminess in the observational record has so far yielded inconclusive results, probably due to the difficulty of constructing*

homogeneous series of wind speed, because of e.g. station relocation or changing measuring techniques. Furthermore, the covered period might be too short to realistically demonstrate trends in the rarely occurring extreme wind events.

Old version: *The analysis of long-term trends in wind extremes and storminess in the observational record has so far yielded inconclusive results, probably due to the difficulty of constructing homogeneous series of wind speed, because of e.g. station relocation or changing measuring techniques.*

p. 1483, l. 28: There is already a "Nevertheless" in the sentence before, so that this "However" sounds weird.

We removed "However".

p. 1484, l. 1-3: I also think that topographic feature may play a role within regional simulation as compared to coarse global models.

New version: *In this respect, regional climate models, driven by the fields simulated by global climate models, should provide a better representation of small-scale processes, topographic influences and of the land-sea contrasts (Gómez-Navarro et al., 2015b; Hall, 2014; Gómez-Navarro et al., 2013), and thus they should be better suited for the simulation of extreme events.*

Old version: R*egional climate models, driven by the fields simulated by global climate models, should provide a better representation of small-scale processes and of the land-sea contrasts (Hall, 2014), and thus they should be better suited for the simulation of extreme events.*

p. 1484, l. 7-13: Please clarify here that you mainly differentiate global and regional climate models.

New version: *In this study we present an analysis of the variability of daily wind speed statistics over Northern Europe over the past centuries as simulated by different regional and global climate models.*

Old version: *In this study we present an analysis of the variability of daily wind speed statistics over Northern Europe over the past centuries as simulated by different climate models.*

p. 1484, l. 22: This first sentence is not very precise. What do you mean by "mean"? spatial or temporal?

New version: *Our study focuses on the statistical relationship between spatial and temporal mean temperature/pressure and daily wind statistics.*

Old version: *Our study focuses on the statistical relationship between mean temperature/pressure and daily wind statistics.*

p. 1485, l. 28: There misses a space at "Roeckner et al."

We included the missing space.

p. 1486, l. 7: I think there is a capital for Earth. There is also a missing ""s" afterwards

The reviewer is right, we changed this.

p. 1486, l. 21-25: More description of the forcing is necessary. What are the differences of forcings between all the simulations? I assume they may not use the same solar forcing, for instance between the very old run from ECHOG and the recent one from ECHAM6 (but maybe I'm wrong, please clarify).

We included a new subsection: "External forcings of the GCMs", which includes a table and a brief comparison of the forcing differences for ECHO-G, ECHAM5 and ECHAM6.

p. 1487, l. 6-8: Does the regional models also use the same land-use change interpolated at their grid scale? I assume so, but it is worth better clarifying that. Maybe a table describing the external forcing for each simulation could be useful. Moreover, I cannot find any precise information concerning the exact domain of the regional models, and we need this (can be indicated in one of the tables for instance).

Yes, the same forcings as in their driving GCM are included in the RCM simulations. We included this information by:
"*Note that for the RCM simulations the same external forcings were applied as for their driving global simulations.*"
We included a new figure indicating the land-sea-masks as well as the RCM domains for CCLM, MM5 and coastDat2.

p. 1487,l. 26: Why do you say "also", while you do not state before that former reanalysis use spectral nudging from von Storch. This does not sound logical. Please clarify logical connection.

The reviewer is right, this is confusing. We removed this part. The sentence now reads as follows:

New version: *In addition we analyse the high resolution regional product coastDat2 (Geyer, 2014) resulting from a simulation with the regional model CCLM and driven by the global NCEP/NCAR reanalysis using a spectral nudging technique (after von Storch et al. (2000)).*

Old version: *In addition we analyse the high resolution regional product coastDat2 (Geyer, 2014) resulting from a simulation with the regional model CCLM and driven by the global NCEP/NCAR reanalysis using also the same spectral nudging technique (after von Storch et al., 2000).*

p. 1489, l. 1: This definition for the gradient is not very precise. Please give the exact boundary of the box used.

We added:
Due to the different resolutions the exact geographical domains of N and S differ. Therefore the border between both varies from around 53°N to 57°N.

p. 1494, l. 28: what is "(s."?

We removed all "s.".

p. 1496, l. 19: Can you give a flavour of what this "underlying physical mechanism" is? (Please be more precise).

New version: As *already known by the scientific community NAO and mTemp are correlated, hence it is not surprising that in most simulations both show comparable relations to the wind speed distribution. Nevertheless, due to internal model variability and different resolutions the global and regional models show different spatial fingerprints for the correlation maps.*

Old version: *Thus, the relationships between STD and the NAO and the relationship between STD and mTemp are similar, suggesting that both are a reflection of the same underlying physical phenomenon. However, this underlying link has a different spatial fingerprint in the regional models and in the global models.*

p. 1499, l. 9: Fig. 6 appears before Fig. 5 I think.

We changed this order.

p. 1500, l. 9: What about other time period?

We included the analysis of another time period from 1571 to 1690:
New version: *The spatial agreement between the reduction in tree fraction and the widening of the wind speed distribution between the beginning and the end of the millennium is remarkable and strongly supports the hypothesis that the distribution of wind speed is mainly affected by land-use changes and related changes in surface roughness length.*
This is supported by the analysis of a third time period from 1571 to 1690 AD (P3) which also shows a strong agreement for the STD ratio (P3/P2; Fig. 10c) and the tree fraction difference (P3-P2; Fig. 10d), albeit with less intense values presumably due to the less intense deforestation in period P3. Hence, we conclude that a less extensive forest cover causes a widening of the wind speed distribution, and vice versa.

Old version: *The spatial agreement between the reduction in tree fraction and the widening of the wind speed distribution between the beginning and the end of the millennium is remarkable and strongly supports the hypothesis that the distribution of wind speed is mainly affected by land-use changes and related changes in surface roughness length. A less extensive forest cover causes a widening of the wind speed distribution, and vice versa.*

p. 1500, l. 15-18: Indeed, but this is a strong caveat, that should be analysed in more depth.

We extended this analysis by plotting the tree fraction time series which shows that this is a slow trend which only has an effect on multi-centennial time scales. Additionally we show the correlation between mTemp and STD for the periods P1 and P2. Due to the shorter time covered in these periods the tree fraction is insignificant.

New version: *Therefore, at multi-centennial timescales the correlation between the wind speed distribution and temperature that was explored in the previous sections could have been indirectly caused by landuse changes. At these timescales, anthropogenic deforestation and mean temperature exhibit a positive trend. Thus the expansion of the wind speed distribution and the increase of temperature in these decades might be induced by physically different factors, leading to positive correlations in our analysis. Figure 11a shows the temporal evolution of the tree fraction used to drive ECHAM5 and ECHAM6 (black line). This proves that on shorter time scales (e.g. 100 or 200 years) the effect of this surface-boundary process is negligible, especially before the 17th century when the*

trend is very weak. Figures 11b+c exhibit the correlation between mTemp and the STD for the periods P1 and P2 calculated with a 5 year running mean. Hence, these figures show the relationship between mean temperature and the wind speed distribution independent of the deforestation effect.

Old version: *Therefore, at centennial timescales the correlation between the wind speed distribution and temperature that was explored in the previous sections could have been indirectly caused by land-use changes. At these timescales, anthropogenic deforestation and mean temperature exhibit a positive trend.*

Fig. 1-4: Please use the same time period when comparing different correlations, at least to check sensitivity of the results to the time period considered. So: recent period when including reanalysis and no reanalysis for period before. Maybe, this will give the same results, but this will be more robust and rigorous (role of forcing, stationarity...) to evaluate this sensitivity.

We extended our analysis for the two overlapping time periods without reanalysis data (1655-1990) and with reanalysis data (1948-1990). We re-calculated the correlation values for Table 2 and re-plotted figures 1 to 4. A new subsection describes the differences between those time periods and two new figures show the results for 1948-1990 for mTemp-P50 and mTemp-STD.

Fig. 5: The legend is not precise enough. Are any smooth applied? Remind the region for the average, can we have an idea of the forcing (I have the impression for instance that Samalas volcanic eruption forcing was far larger in ECHAM5 than in the other, or maybe this is just due to stronger dynamical response)?

We excluded this figure as Referee #1 pointed to the fact that two of these time series are also included in figure 6.
Nevertheless, to answer your question, ECHAM5 and ECHAM6 include comparable forcings, hence the mentioned relation to the Samalas eruption likely occurs by chance as it is only visible in ECHAM5. We conclude that this difference between ECHAM5 and ECHAM6 is due to internal model variability.

Fig. 7: Please show other period as well.

We added a third period from 1571 to 1690 (P3).

Additional Information: Please note that during the revision of the manuscript we realised that we had accidentally used a different ECHAM5 simulation than the one that had been in fact used to drive the model CCLM. We used the ECHAM5-E1 run, which differs from the actual CCLM driving version ECHAM5-E2 only in a weaker solar forcing. Our conclusions do not change.

Variability of daily winter wind speed distribution over Northern Europe during the past millennium in regional and global climate simulations.

S. E. Bierstedt[1], B. Hünicke[1], E. Zorita[1], S. Wagner[1], and J. J. Gómez-Navarro[2]

[1]Institute of Coastal Research, Helmholtz-Zentrum Geesthacht, Geesthacht, Germany
[2]Climate and Environmental Physics, Physics Institute and Oeschger Centre for Climate Change Research, University of Bern, Switzerland

Correspondence to: Svenja Bierstedt (svenja.bierstedt@hzg.de)

Abstract. We analyse the variability of the probability distribution of daily wind speed in wintertime over Northern and Central Europe in a series of global and regional climate simulations covering the last centuries, and in reanalysis products covering approximately the last 60 years. The focus of the study lies ~~in~~ on identifying the link ~~between~~ of the variations in the wind speed distribution to the

5 regional near-surface temperature, to the meridional temperature gradient and to the North Atlantic Oscillation.

The climate simulations comprise three simulations, each conducted with a global climate model that includes a different version of the atmospheric model ECHAM. Two of these global simulations have been ~~regionalised~~ downscaled with the regional climate models MM5 and CCLM. The

10 reanalysis products are the global NCEP/NCAR meteorological reanalysis version 1 and a regional reanalysis conducted with a regional atmospheric model driven at its domain boundaries by the NCEP/NCAR reanalysis.

Our main result is that the link between the daily wind distribution and the regional climate drivers is strongly model dependent. The global models tend to behave similarly, although they show some dis-

15 crepancies. The two regional models also tend to behave similarly to each other, but surprisingly the results derived from each regional model strongly deviates from the results derived from its driving global model. The links between wind speed and large-scale drivers derived from the reanalysis data sets overall tend to resemble those of the global models. In addition, considering multi-centennial time scales, we find in two global simulations a long term tendency for the probability distribution of

20 daily wind speed to widen through the last centuries. The cause for this widening is likely the effect of the deforestation prescribed in these simulations.

We conclude that no clear systematic relationship between the mean temperature, the temperature

gradient and/or the North Atlantic Oscillation, with the daily wind speed statistics can be inferred from these simulations. The understanding of past and future changes in the distribution of wind speeds, and thus of wind speed extremes, will require a detailed analysis of the representation of the interaction between large-scale and small-scale dynamics.

1 Introduction

Anthropogenic climate change is expected to cause an increase of various types of extreme events, such as heat waves, but its effects on extreme winds is less clear. Indeed, Chapter 3 of the Intergovernmental Panel on Climate Change (IPCC) special report 'Managing the Risks of Extreme Events and Disasters to Advance Climate Change Adaptation' states that there is only low confidence in projections of changes in extreme winds (Seneviratne et al., 2012). One way to reduce this uncertainty is to compare the output of paleoclimate simulations over the past centuries with empirical evidence of past wind conditions, for instance derived from historical evidence or natural proxies (Costas, 2013). While there is still a dearth of proxy records reflecting past changes in wind speed, new types of proxy records are being developed (Costas, 2013). A precondition for this comparison is to test whether different climate models provide a consistent picture of past changes in wind speed distribution. In this study we analyse several simulations with global and regional models and investigate to what extent they provide a consistent ~~view~~ picture of the relationship between the variations in the wind speed distribution and large-scale drivers. We focus on Northern Europe in wintertime as this region and season are particularly prone to storminess.

Hypotheses put forward to explain changes in storminess are related to the general physical consideration that warmer periods provide more humidity and consequently more (latent) energy for possible storms. However, warmer periods are generally characterized by a weaker meridional temperature gradient due to the stronger warming of the high latitudes with respect to the tropics, and thus a weaker baroclinicity, which should lead to weaker or less storms (Li and Woollings, 2014; Yin, 2005). In addition, the North Atlantic Oscillation (NAO), as the main pattern of troposphere dynamics over the North Atlantic-European sector, is also related to the interannual variability of seasonal mean winds in this region. It is thus very plausible that ~~it~~ the NAO is also involved in the variations of the distribution of daily wind speeds, e.g. Wang et al. (2011) state that NAO variations show a relationship with the 99th percentile of wind speed. The NAO itself could also be related to changes in ~~temperature~~European near-surface winter temperature (Rutgersson et al., 2015). In this regard, scenario simulations ~~in general indicate a tendency towards a stronger meridian pressure gradient in the future , but the~~ indicate a contradicting tendency of the NAO in a warmer future, depending on whether it is defined from the sea-level pressure (SLP) gradient or from the geopotential height at 500 mbar (Z500). Gillett and Fyfe (2013) showed that the meridional SLP gradient will tend to become steeper polewards. On the other hand Cattiaux and Cassou (2013) also found a positive trend of the

2

SLP gradient but found a negative trend of the Z500 gradient. Our study focuses on surface winds which are rather influenced by SLP variations. The link between the NAO and external climate forc-
ing over the past centuries is, however, unclear in climate simulations (Gómez-Navarro and Zorita, 2013).

Thus, for Northern Europe, from the dynamical point of view it is not clear how the distribution of wind speed would respond to changes in temperature. The analysis of long-term trends in wind extremes and storminess in the observational record has so far yielded inconclusive results, proba-
bly due to the difficulty of constructing homogeneous series of wind speed, because of e.g. station relocation or changing measuring techniques. Furthermore, the covered period might be too short to realistically demonstrate trends in the rarely occurring extreme wind events. On the other hand, re-
analysis products covering long periods (e.g. the 20th Century Reanalysis 20CR,)(e.g. the 20th Cen-
tury Reanalysis 20CR; Compo et al., 2011) may be inhomogeneous due to the assimilation of new types of data through the simulated period. There has been a considerable debate on the storminess trends in long-term reanalysis data sets (Brönnimann et al., 2012; Krueger et al., 2013; Wang et al., 2013). Krueger et al. (2013) stated that before 1950 the time series of 20CR and observational mean sea level pressure are not consistent. They suggested that the increasing station density density of station data leads to these inconsistencies. Wang et al. (2013), on the other hand, argued that new measurement errors and changed sampling frequencies would produce these inhomogeneities. This debate has also been discussed by Feser et al. (2015), who concluded that the analysis of long-term reanalysis data, affected by changing station density, should be conducted with caution.

The analysis of the climate of the past centuries can shed light on the question whether external cli-
mate forcing has an effect on the intensity or frequency of wind extremes and whether or not the tem-
perature variability is linked to variability in statistics of wind speeds. Unfortunately, proxy-based climate reconstructions in general still do not provide information about extreme wind statistics in the past, except for intense tropical cyclones (e.g.)(e.g. Donnelly and Woodruff, 2007). However, new types of proxy data that may record past wind speed are being retrieved. For instance, coastal dunes at the North Sea coast contain layered structures that can be analysed by ground-penetrating radar. The layered structures contain information about grain size distribution and, indirectly, about intensity or frequency of high winds in the past (Costas, 2013). These types of proxies can poten-
tially be used to test the skill of climate models to simulate the relationships between extreme wind statistics and external forcing or between extreme wind statistics and low-frequency variability of the large-scale surface climate.

The evolution of temperatures of the past millennium in this region, as reconstructed from proxy and long-instrumental records, exhibits a generally warm period in the early centuries (the Medieval Warm Period) and generally colder centuries around 1700 AD (the Little Ice Age), with the subse-
quent warming leading to the current recent warm period (Luterbacher et al., 2004; 2k Consortium, 2013; Esper et al., 2014). This alternation of warm and cold periods has been likely caused by ex-

ternal climate forcings (Hunt, 2006; Fernandez-Donado et al., 2013), in particular the recent warm period and the Little Ice Age, and thus it provides a suitable test of whether the variability of extreme wind statistics may follow a similar alternation.

Climate simulations had been previously used to address the connection between winds and temperatures in the past ~~(e.g.)~~(e.g. Fischer-Bruns et al., 2005; Schimanke et al., 2012). Fischer-Bruns et al. (2005) analysed two historical climate simulations with the global climate model ECHO-G covering the period from 1550 to 1990 AD. These authors found that storminess and large-scale temperature variations were mostly decoupled in these simulations. However, they ~~mentioned~~ reported a connection between storm track variability and temperature over the North Atlantic for one of the two simulations in two periods with extremely low external forcing, namely the Late Maunder Minimum (1675–1710 AD) and the Dalton Minimum (1790–1840 AD). Nevertheless, they found no evidence of a linear co-variation between the number of extra-tropical storms and temperature variations in the simulations analysed.

~~However, the~~ The spatial resolution of global climate models may not be adequate to realistically represent extreme events, especially over regions with complex coastlines. ~~Regional~~ In this respect, regional climate models, driven by the fields simulated by global climate models, should provide a better representation of small-scale processes, topographic influences and of the land-sea contrasts (Gómez-Navarro et al., 2015b; Hall, 2014; Gómez-Navarro et al., 2013), and thus they should be better suited for the simulation of extreme events. Nevertheless, despite the fact that regional models provide an added value (Feser et al., 2011) they are also bound by the circulation biases of the driving global climate model simulations (Hall, 2014).

In this study we present an analysis of the variability of daily wind speed statistics over Northern Europe over the past centuries as simulated by different regional and global climate models. We mainly focus on the consistency among the different models in simulating the relationship between large-scale drivers and the statistics of daily wind speed with the goal of identifying robust patterns across models that can be later tested with proxy reconstructions.~~Our main result indicates that climate models provide still ambiguous answers, which should be reconciled first.~~

This paper is structured as follows: Chapter 2 describes the analysed data sets separated into climate simulations of global circulation models, regional circulation models and reanalysis products. Chapter 3 defines our area of interest and outlines the applied methods and definitions. Chapter 4 presents the analysis of the relationship of large-scale drivers and wind speed variance, as well as the comparison of the evolution of the wind speed variance in the millennium simulations. A discussion of the results and conclusions closes the manuscript.

2 Data

Our study focuses on the statistical relationship between spatial and temporal mean temperature/pressure and daily wind statistics. We use monthly mean two-meter temperature (T2M) values, monthly mean values of mean sea level pressure (MSLP) and daily mean 10-meter wind speed (WS) for our analysis. These values are taken from a set of five simulations performed with five different models, with different spatial and temporal resolution: two simulations with the Regional Climate Models (RCMs) MM5 and CCLM, and three simulations with the global General Circulation Models (GCMs) ECHAM4-HOPE-G, ECHAM5/MPI-OM and ECHAM6/MPI-OM. ECHAM4-HOPE-G and ECHAM5-MPIOM were chosen because they had been used as the boundary forcing for the two RCM simulations, respectively. Note that for the RCM simulations the same external forcings were applied as for their driving global simulations. ECHAM6/MPI-OM was chosen due to its higher spatial resolution similar to the resolution of the RCM simulations analysed, but also for being the next generation of the previous versions of ECHAM4 and ECHAM5. Additionally, we analyse the global reanalysis NCEP/NCAR version 1 and ~~the regional reanalysis~~ a regional reanalysis named coastDat2. Table 1 summarizes the information about spatial and temporal resolution and time periods of the data sets used. Figure 1 shows the land-sea-masks for all data sets. For the regional data sets (CCLM, MM5, coastDat2) the whole available domain is visible and the study area is marked by a red rectangle. In the following we introduce the different data sets in more detail and describe their main differences.

2.1 Global Climate Model simulations

The coupled GCM ECHAM4-HOPE-G, also denoted in previous literature as ECHO-G (Legutke and Voss, 1999) consists of the atmospheric component (AGCM) ECHAM4 (Roeckner et al., 1996) and the ocean-ice component (OGCM) HOPE-G (Wolff et al., 1997). ECHAM4 has a horizontal resolution of T30 (approx. $3.75°\text{x}3.75°$, $\approx$ 400 km x 260 km in high mid-latitudes) and 19 vertical levels and HOPE-G a horizontal resolution corresponding to T42 (approx. $2.8°\text{x}2.8°$, $\approx$ 300 km x 200 km in high mid-latitudes) and 20 vertical levels. Both sub-models have been developed at the Max Planck Institute for Meteorology (MPI-M) in Hamburg. The ~~analysed~~ ECHO-G millennium simulation (1001-1990 AD) is part of an ensemble of simulations conducted by the Helmholtz-Zentrum Geesthacht (HZG). The simulation is forced with changes in total solar irradiance, the dimming effect of volcanic eruptions on solar irradiance, and changes in greenhouse gases (CO_2, NO_2, CH_4). The simulation was started with a cold ocean initial condition taken from a previous simulation corresponding to a situation representative of the Little Ice Age (Hünicke et al., 2011; von Storch et al., 2004; Zorita et al., 2004).

The coupled GCM ECHAM5/MPI-OM consists of the atmospheric component ECHAM5 ~~(successor of ECHAM4,)~~ (successor of ECHAM4, Roeckner et al., 2003) and the ocean and sea-ice com-

ponent MPI-OM (Marsland et al., 2003). ECHAM5 has a T31 resolution with 31 vertical levels. The MPI-OM component has a horizontal resolution corresponding to T42 and 23 vertical levels.

165 The analysed simulation ECHAM5/MPI-OM (850-2005 AD) is part of an ensemble of simulations conducted by the Max-Planck-Institute for Meteorology in Hamburg and will hereafter simply be named ECHAM5. It is driven by changes in solar irradiance (Bard et al., 2000), volcanic eruptions (Crowley et al., 2008), changes in ~~earth'~~Earth's orbital parameters, greenhouse gas and aerosol forcings. Additionally, land cover changes (Pongratz et al., 2008) are considered in this simulation. More

170 details about the simulation setup and forcings can be found in Jungclaus et al. (2010).

We also include a climate simulation with the model MPI-ESM with the P configuration ~~(MPI-ESM-P,)~~(MPI-ESM-P, Giorgetta et al., 2013), which consist of the successor of ECHAM5 and the newest version of ECHAM, named ECHAM6 (850-2005 AD). The main differences between ECHAM6 and ECHAM5 are the higher vertical resolution (i.e., 47 instead of 31 vertical levels), increased horizon-

175 tal resolution of T63 ($1.875° \times 1.875°$, $\approx$ 200 km x 130 km in high mid-latitudes), the incorporation of new aerosol and surface albedo climatology and the use of a new shortwave radiation scheme in ECHAM6 (Crueger et al., 2013). The MPI-ESM-P simulation is part of the Climate Model Intercomparsion Project version 5 ~~(CMIP5,)~~(CMIP5, Taylor et al., 2012). The boundary layer and turbulence parametrization in ECHAM6 is based on the eddy diffusivity/viscosity approach (Stevens et al.,

180 2013). The model was driven by changes in greenhouse gases and spectrally resolved solar irradiance, volcanic activity (Crowley et al., 2008), changes in ~~earth'~~Earth's orbital parameters and land use changes (Pongratz et al., 2008).

2.2 External forcings of the GCMs

We outlined above the key-properties of the analysed global simulations. However, the differences
185 in the external forcings used to drive the simulations play a crucial role in our analysis. Hence, we additionally provide a comparison of these differences. An overview can be found in Table 2. A more comprehensive comparison between ECHO-G and ECHAM5 was given by (Fernandez-Donado et al., 2013), however, we summarise it here and extend it for ECHAM6.

While all three simulations include total solar irradiance (TSI), greenhouse gas (GHG) and volcanic
190 forcing as external forcings, only ECHAM5 and ECHAM6 ~~are the only simulations included in this analysis forced with land use changes~~ incorporate also anthropogenic aerosols and land use changes. There are various estimations of past TSI, which can be broadly divided into a strong (S; >0.2% TSI change since the Late Maunder Minimum (LMM)) and a weak (s; <0.1% TSI change since LMM) amplitude of variations (Fernandez-Donado et al., 2013). Strong (S) solar forcing is
195 applied for ECHO-G and ECHAM5, in which ECHO-G uses higher values than ECHAM5. Weak (s) solar forcing is applied for ECHAM6. Estimations of changes in the main well-mixed GHG concentrations (CO_2, CH_4, N_2O) are obtained from air bubbles enclosed in Antarctic ice cores. The CO_2 concentrations were prescribed in ECHO-G after Etheridge et al. (1996), in ECHAM5 and

6

ECHAM6 they follow Marland et al. (2003). The incorporation of the volcanic forcing into ECHO-G was done by including the net effect of stratospheric volcanic aerosols in an effective solar constant in terms of a reduction in incoming shortwave radiation. For ECHAM5, latitudinally resolved changes in optical depth in the stratosphere were used. This might have an impact on climatic changes due to volcanic eruptions e.g. on the atmospheric circulation, especially over the extratropics during winter (see Fernandez-Donado et al. (2013) and included references). The orbital changes and land-use changes (only included in ECHAM5 and ECHAM6) are the same in both simulations. Orbital variations follow Bretagnon and Francou (1988) and vegetation changes Pongratz et al. (2008).

2.3   Regional Climate Model simulations

The RCM MM5 model consists of a slight modification of the non-hydrostatic Fifth-generation Pennsylvania-State University-National Center for Atmospheric Research Mesoscale Model. Such modification allows this meteorological model to perform long climate simulations. This setup has been used to conduct a long high-resolution climate simulation of the European climate during the last millennium, driven at the domain boundaries by the coupled GCM ECHO-G (Gómez-Navarro et al., 2013, 2015a). For the planetary boundary layer formation parametrization, this simulation ~~uses~~ used the medium-range forecast ~~(MRF,)~~ (MRF, Hong and Pan, 1996) scheme. The RCM was driven by the same set of external forcing as the driving GCM ECHO-G (~~s.~~ Sect. 2.1) to avoid physical inconsistencies. The domain of MM5 has a spatial resolution of ~~0.5°x0.5° (≈ 70 km x 40 km)~~45 km. The model output is available on a daily scale and covers the period 1001–1990 AD. The analysed millennium simulation MM5-ECHO-G will hereafter be named MM5.

A second regional simulation ~~is~~ was carried out with the non-hydrostatic operational weather prediction model COSMO in CLimate Mode (CCLM) (Rockel and Hense, 2008). The CCLM model ~~is~~ was driven by initial and boundary conditions of the global ECHAM5 simulation. The regional model ~~is~~was, however, free to produce its own small scale spatial variability. The COSMO model uses a boundary layer approximation by implying horizontal homogeneity of variables and fluxes, which ignores all horizontal turbulent fluxes (Doms et al., 2011). The CCLM simulation over Europe ~~has~~ had roughly the same spatial resolution as the MM5 simulation, but it covers only the period from 1655 to 1999 AD. The simulation CCLM-ECHAM5 will hereafter be abbreviated as CCLM.

2.4   Reanalysis Data

The NCEP/NCAR reanalysis covers the period from 1948-present and has a spatial resolution of $2.5°$ ($\approx$ 270 km x 175 km in high mid-latitudes) with 28 levels and is available at 6-hourly intervals (Kalnay and Coauthors, 1996; Kistler and Coauthors, 2001). In addition we analyse the high resolution regional product coastDat2 (Geyer, 2014) resulting from a simulation with the regional model CCLM and driven by the global NCEP/NCAR reanalysis using ~~also the same~~ a spectral nudging technique ~~(after)~~(after von Storch et al., 2000). The regional reanalysis coastDat2 covers Europe

7

and the North Atlantic for the period from 1948 to present. It has a spatial resolution of $0.22°$ (≈ 25
km x 15 km) and the output is available on hourly time intervals. ~~This data set will be denoted in the following coastDat2.~~

All wind speed data were daily averaged to proceed with the analysis.

~~Overview of the analysed simulations/reanalysis and their simulation acronyms, underlying atmosphere and ocean models, boundary forcings (only for regional data sets) as well as the spatial resolution of the atmosphere models and time periods, as used for the analysis. Simulation Atmosphere Ocean Boundary atm. spatial res. Vegetation PeriodGCM ECHO-G ECHAM4 HOPE-G 3.75° constant 1001-1990ECHAM5 ECHAM5 MPI-OM 3.75° time dependent 850-2005ECHAM6 ECHAM6 MPI-OM 3.75° time dependent 850-2005RCM MM5 MM5 ECHO-G 0.5° constant 1001-1990CCLM CCLM ECHAM5 0.5° constant 1655-1999Reanalysis coastDat2 CCLM* NCEP 0.22° constant 1948-2012NCEP 2.5°constant 1948-2012~~

3   Methods and definitions

Our analysis concentrates on the distribution of daily wind speed in wintertime (December, January, February - DJF) over central and northern Europe. The area of investigation has approximately the same extension from $45°$ to $65°$N and $0°$ to $30°$E for all data sets analysed.

The statistics of daily wind speed were evaluated over gliding time windows for the different simulation periods. These wind speed statistics include the standard deviation (STD) of the distribution, its 50th, 95th and 99th percentiles (P50, P95, P99) and the differences P95 minus P50 (diffM) and P99 minus P95 (diffE) as a measure of the width of the distribution in the high wind ranges. The analysis of several percentiles and their differences allows the determination of basic changes in the characteristics of wind speed distributions, hence it is possible to investigate if it shifts with time with unchanged shape and/or whether its width changes. Thus, we can discriminate between a change in the mean and/or in the extreme of the wind speed distribution. In our case 'extreme' means the tail of the distribution, which includes values above the 95th percentile. For instance, increasing diffM and diffE values would show a broadening of the distribution which means higher extreme wind speeds. The three climate parameters analysed regarding their influence on wind speed are (1) mean seasonal near-surface air temperature (mTemp), (2) mean seasonal meridional temperature gradient (tGrad) and (3) the North Atlantic Oscillation index (NAO).

The temperature gradient is calculated as the absolute value of the difference between the northern (N) and the southern (S) half of the investigation area $tGrad = abs(N - S)$ for each model simulation. Due to the different resolutions the exact geographical domains of N and S differ. Therefore the border between both varies from around 53°N to 57°N.

The North Atlantic Oscillation (NAO) index is defined as the leading pattern resulting from principal component analysis (PCA) of the winter mean sea-level pressure (MSLP) field. This dominant

pattern of variability is characterized by a low pressure system over Iceland and a high pressure system over the Azores (exemplarily shown for ECHAM6 in Fig. 2). As MSLP field we used the GCM gridded pressure information of the North Atlantic and European area. This domain approximately spans from 70°W to 30°E longitude (from ≈ Boston to Istanbul) and from 70°N to 20°N latitude (from ≈ Tromsø to the southern part of Morocco). For computations conducted for the RCM simulations we used the NAO patterns derived from the driving GCM fields as well.

Because we are interested in the relationship between the slowly changing mean climate and the variability of the distribution of daily wind speed, the wind statistics are calculated considering gliding time windows over the respective time series for each model simulation before they are correlated with the running mean values of the atmospheric drivers. The climate parameters analysed are considered as means over the respective time windows and for Figures 3-8 these values are spatially averaged before the correlation computation with the wind statistics. For the long climate model simulations (ECHO-G, ECHAM5, ECHAM6, MM5, CCLM) we use 30-year running windows and for the shorter reanalysis data (coastDat2, NCEP) 5-year running time windows.

The temperature gradient is calculated as the absolute value of the difference between the northern (N) and the southern (S) half of the investigation area $tGrad = abs(N - S)$ for each model simulation. The North Atlantic Oscillation (NAO) index is defined as the leading pattern resulting from principal component analysis (PCA) of the winter mean sea-level pressure (MSLP) field. This dominant pattern of variability is characterized in all simulations by a low pressure system over Iceland and a high pressure system over the Azores.

Test for significance: Random-phase bootstrap

3.1 Test for significance: Random-phase bootstrap

A random-phase bootstrap method (Schreiber and Schmitz, 1996; Ebisuzaki, 1997) is applied to determine the significance of the correlation coefficients shown in Table 3 with a significance level of p=0.05. This method allows us to take into account the autocorrelation structure of the series. For this method a Fourier transformation of the time series is conducted. The phases of the Fourier-transformed series are then replaced by random phases, and the result is transformed back to the time domain to obtain new surrogate time series. The surrogate time series has the same spectrum and autocorrelation as the original time series, but has a random time evolution. By generating a large number of surrogate time series, an empirical distribution of the correlation coefficient under the null-hypothesis (that the correlation is zero) can be constructed and used to determine the statistical significance of the correlation coefficient.

4 Results

As previously mentioned, this study is based on correlations between different parameters of the probability distribution of daily mean wind in wintertime and selected potential drivers: mean seasonal near-surface air temperature (mTemp), mean seasonal meridional temperature gradient (tGrad) and North Atlantic Oscillation index (NAO). Table 3 presents a summary of the statistical relationships derived from the different model simulations analysed. The presented time correlation coefficients are obtained by calculating the parameters of the daily wind probability distribution at grid-cell scale, followed by averaging over the whole spatial domain. The spatially resolved statistical analysis is presented for each model in the following sections. The significance of the correlation coefficients presented in Table 3 is tested as described in Sect. 3 3.1 by a random phased bootstrap method phase bootstrap method (Schreiber and Schmitz, 1996; Ebisuzaki, 1997) and marked as bold characters.

In the following, we first present the general findings for each of the climate drivers analysed (mTemp, tGrad, NAO) by comparing all considered model simulations and reanalysis products. This is followed by a more detailed presentation of the results with focus on (a) the regional model simulations and their corresponding driving global models (b) the simulation with the global model ECHAM6/MPI-OM and (c) the reanalysis products. In addition, (d) we compare the results for the overlapping time periods without reanalysis (1655-1990 AD) and with reanalysis (1948-1990 AD) data and (e) for some of the long simulations a comparison of time slices is presented.

4.1 General comparison of all data sets

Relationship between mTemp and tGrad

A common characteristic shared by all analysed simulations is the negative correlation between the mean winter temperature (mTemp) and the mean meridional temperature gradient (tGrad). Hence, in warmer decades the northern regions warm more strongly than the southern regions, and in colder decades the northern regions also cool more strongly than the southern regions. This 'high-latitude amplification' is also found in climate simulations for future scenarios. In those simulations, it is caused by several positive feedbacks that operate more strongly at high latitudes, such as ice-snow-albedo feedback (Hall and Qu, 2006) and black-body radiation feedback (Pithan and Mauritsen, 2014). European temperature reconstructions over the past centuries also indicate that in colder periods such as the Late Maunder Minimum (around 1700 AD) temperatures in higher latitudes cooled down more strongly than further south (Luterbacher et al., 2002).

Relationship between mTemp and wind speeds

The relationship between the mTemp and the median winds (P50) is positive in all analysed simulations and reanalysis products, with the exception of the regional simulation with MM5. The correlations, taken individually, are not always statistically significant at the 5% level. These positive

10

correlations imply that periods with higher winter temperatures than normal also tend to show higher median winds. Contrary to the rest of the simulations and also opposite to the link found in its driving global model ECHO-G, the particular behavior of the regional model MM5 is not limited to this
340 particular correlation between mean air temperature and median wind. Table 3 already shows that the MM5 simulation often behaves differently compared to all other simulations. The other regional model CCLM does show a positive correlation between air temperature and median wind, but this correlation is lower compared to the global simulations and in the reanalysis products.

Warmer air temperatures are also strongly linked to larger values of the high percentiles of the dis-
345 tribution of daily wind, P90 and P95 and P99, for most of the simulations. Again, the exceptions relate to the regional model simulations MM5 and CCLM. MM5 presents a negative correlation and CCLM a weak positive correlation.

Variations in the width of the daily wind distribution are described by the differences between the high percentiles, P90 or P95 or P99, and the median wind P50. The correlations between these mea-
350 sures of the distribution widths and mean temperature tend to be small for all simulations with the exceptions of the regional models MM5 and CCLM. For these two regional models the correlations are strongly negative, and more strongly so for the MM5 model, indicating that in periods with warmer air temperatures the wind distribution gets narrower at the same time that it shifts to lower values of wind speed, as indicated by the negative correlation with P50.

355 Relationship between tGrad and wind speeds

The correlation coefficients between the distribution of wind speeds and tGrad are summarized in the second third block of Table 3. In general, the correlations tend to be weak, with some exceptions. In the MM5 simulations they are stronger and positive, whereas in the ECHAM6 simulation they are somewhat weaker but negative. Both reanalysis products also offer a contrasting picture. In the
360 NCEP reanalysis the correlations between tGrad and the median wind P50 or the higher percentile winds P90 and P95 and P99 are negative and statistically significant, whereas in the coastDat2 product they tend to be positive but weak.

Relationship between NAO and wind speeds

The NAO is a large-scale winter circulation pattern that describes the mean strength of the seasonal
365 mean westerly winds in the North Atlantic-European sector and therefore it is plausible that it is also related to the distribution of the daily wind speed in Northern Europe. The correlations between the NAO index across the different simulations yield, however, an incoherent picture. Most simulations display a positive and relatively strong correlation between the NAO index and the spatially averaged P50, with the exception of the two regional models, MM5 and CCLM.

370 Thus, the regional models behave again different differently to their respective driving GCMs. In the case of MM5 the correlation between the NAO index and P50 correlation is strikingly negative whereas in the case of CCLM the correlation is weakly positive. A positive phase of the NAO is linked to stronger westerly winds over Northern Europe and hence a negative or weakly negative

correlation of the NAO with P50 is surprising. We show later that the negative sign of this corre-
lation in the regional simulations is caused by the behavior of the regional models over land areas,
whereas the sign of the correlation over ocean is the expected one.

The correlation between the NAO index and the width of the distribution (STD) of wind speed av-
eraged over the study region tends to be also positive for most simulations, indicating that stronger
mean westerlies tend to concur with a wider distribution of daily wind speed. However, there are
exceptions. Again, the regional model simulation MM5 displays a strong negative correlation and
the regional model simulation CCLM shows a positive but weak correlation. These negative (MM5)
or positive but weak (CCLM) correlations also contrast with the link between the NAO index and
the width of the wind speed distribution in their parent global models, ECHO-G and ECHAM5,
respectively, both of which display positive and statistically significant correlations. Similarly to the
global models, in both reanalysis products the NAO index is strongly and positively correlated with
the width of the wind speed distribution.

Relationship between NAO and mTemp

It is well known that the winter NAO index is positively correlated with air temperatures in Northern
Europe. The link between the parameters of the wind speed distribution on one side, and the NAO
or the mean air temperature on the other side may thus be just a reflection of the same physical rela-
tionship. This is also supported by paying attention to how the correlations with the NAO and with
the mean temperature vary across simulations (~~last two lines~~ third line in Table 3). It seems clear that
~~both lines~~ this line in the table ~~display~~ displays a similar, though not identical, pattern of correlations
across the simulations analysed. However, the spatially aggregated analysis does not allow to disen-
tangle which of both factors, NAO or mTemp, is the physical driving factor for the variations in the
distribution of wind speed.

Relationship between mTemp, tGrad and wind speed

The correlations shown in Table 3 are indicative of a simple relationship between mTemp or tGrad
on one side and median wind speed or the width of its probability distribution on the other side.
Certainly, there must be other underlying factors that require a more detailed analysis. For instance,
the period covered by the different data products is different. The reanalysis products represent the
last decades, when the anthropogenic warming is probably dominating temperature trends.

In the following subsections we investigate in more detail the links between the large-scale at-
mospheric drivers and the distributions of daily wind at a grid-cell level, which allows us to better
understand the spatially aggregated correlations included in Table 3. The following figures (Fig. 3-6)
display the correlation patterns between the different large-scale climate indices and the parameters
of the wind speed distribution at grid-cell scale. The upper two panels in the figures show the results
derived from the regional models for direct comparison with their driving GCMs. The lower two

410 panels include the results derived from the GCM ECHAM6 (not used to drive any regional model in
this study) and the two reanalysis products.

4.2 Simulations of the regional models CCLM and MM5 versus their driving global models ECHAM5 and ECHO-G

In the CCLM simulation (1655-1999 AD) the relationship between P50 wind speed and mTemp (Fig.
415 3) in general shows a negative correlation or correlations close to zero, with the exception of a land
area east of the Baltic where the correlation is positive~~(Fig. 3)~~. Hence, in this regional simulation,
colder periods can be related to generally stronger winds. In contrast, the correlation between the
mean temperature and P50 in the ECHAM5 simulation is positive ~~almost everywhere~~in the northern
part of the domain, with some regions showing ~~lower correlations~~ negative correlations in the south,
420 in-between correlations are around zero. The MM5 and the ECHO-G simulations also display a
qualitatively similar, but even more clear, contrast. In the MM5 simulation, median wind speeds
over land areas are clearly negatively correlated with mean temperature, whereas over oceanic areas
P50 is positively correlated with mTemp. The ECHO-G simulation displays clearly positive correla-
tions over the whole area, similar to the ECHAM6 simulation and the regional reanalysis products.
425 Concerning the link between mTemp and the width of the distribution (STD) ~~, both regional models
behave differently to the driving global simulations. In~~ the regional simulations ~~, the STD is negatively
correlated~~ and ECHAM5 the STD correlates negatively with the mean temperature (~~s.~~ Fig. 4a,b and
c), indicating that colder periods tend to be related with a wider distribution of wind speed over the
whole area. This is also supported by the negative correlation between mTemp and the difference
430 P99-P50 (not shown, Table 3). Since P50 in the regional models was also negatively correlated with
mTemp, the regional models tend to be associated with broader wind speed distributions and with
stronger mean winds.

The ~~two driving global simulations display~~ECHO-G simulation (used to drive MM5) displays, in
contrast, positive correlations in a region along the North and South Baltic Sea, straddled by regions
435 of zero or negative correlations in Scandinavia and central Europe (Fig. 4~~b and~~ d).

We assume that ~~this result~~ these results may be induced by a stronger meridional temperature gra-
dient (tGrad; ~~s.~~ see Sect. 3). This assumption is strengthened by the negative correlation between
mTemp and tGrad, which shows a spatially averaged value of -0.56 in the CCLM simulation and
-0.47 in the MM5 simulation. This negative correlation indicates that lower mean temperatures tend
440 to occur with stronger meridional temperature gradients in these simulations, and thus, tGrad could
be the primary driver for the changes in the wind speed distribution. Therefore, we also analysed
the relationship between the parameters of the wind speed distribution and tGrad (Table 3). This
analysis reveals, however, contrasting results between both regional simulations: The correlations in
the CCLM simulation are only minor and not statistically significant, whereas in the case of MM5
445 they are relatively strong for all parameters of the wind speed distribution, except for the difference

13

P99-P50 P99-P95.

We additionally investigate the relationship between the mean NAO index and the distribution of wind speeds. The correlation coefficient between the NAO index (s. Sect. 3) and the median wind P50 displays clear similarities of the regional simulations and the driving global simulations, re-
450 spectively (Fig. 5). However, the differences between the results provided by the regional models and those provided by the global models are profound. The correlation patterns derived from the regional models display positive correlations over oceanic areas, but in general negative correlations over land areas. This is reflected by a west-east correlation dipole (in the CCLM simulations the zero of this dipole does not coincide with the coast line). In contrast, the global simulations display pos-
455 itive correlations over the whole region (Fig. 5b,d,e). The idea that a positive NAO index should be associated with stronger winds in general is only confirmed in the global simulations. The regional models indicate that a stronger NAO tends to be linked to stronger winds only over the ocean and coastal areas, but not over Central and Eastern Europe. This difference may hint to an influence of the boundary layer parametrization in regional models over continental areas.

460 The spatially averaged correlation between the NAO and STD is very low in the CCLM simula-tion (0.12), but much stronger and negative in the MM5 simulation (-0.42). This difference can now be explained by the different correlation patterns shown in Fig. 6a. The spatially resolved map showing the correlation between the NAO index and the grid-cell STD in the regional mod-els CCLM and MM5 and in the global models ECHAM5 and model ECHO-G is remarkably similar
465 to the correlation patterns between the mean temperature and the STD (compare Fig. 6 and 4). Again, the CCLM simulation shows positive correlations over North Western Europe whereas the correlations in MM5 are negative over the whole region. The global models tend model ECHO-G tends to show higher positive correlations over the North Sea and the Southern Baltic Sea, strad-dled by negative correlations over Scandinavia and Central Europe. Thus, the relationships between
470 STD and the NAO and the relationship between STD and mTemp are similar, suggesting that both are a reflection of the same underlying physical phenomenon. However, this underlying link has a different spatial fingerprint in the regional models and in the global models. over Central-Eastern Europe. An exception is the result for ECHAM5, although the spatially averaged correlation between NAO and mTemp shows a high positive value of 0.57 (Table 3), the patterns for mTemp-STD and
475 NAO-STD show completely different signs. A comparison with a different ECHAM5 simulation with a weaker solar forcing (Krivova and Solanki, 2008) showed rather comparable results between mTemp-STD and NAO-STD (not shown). Which leads to the conclusion that the external forcing of each simulation plays a crucial role for the relationship of mTemp and the wind speed distribution. As already known by the scientific community NAO and mTemp are correlated, hence it is not
480 surprising that in most simulations both show comparable relations to the wind speed distribution. Nevertheless, due to internal model variability and different resolutions the global and regional models show different spatial fingerprints for the correlation maps.

14

4.3 The global model ECHAM6/MPIOM

~~ECHAM6 is so far the latest version of the series of atmospheric models including the atmospheric models ECHO-G (ECHAM4/HOPE-G) and ECHAM5. The simulation with ECHAM6 was conducted with a higher spatial resolution, T63 (approximately 1.875°) versus T30/T31 (about 3.75°) for the other two ECHAM versions.~~ In general the correlation patterns between the large-scale drivers and the parameters of the distribution of wind speed resemble those obtained with ECHAM5 and ECHO-G (ECHAM4/HOPE-G), but some clear differences exist. The higher spatial resolution of ECHAM6 does not, however, lead to correlation patterns that resemble those derived from the regional model simulations CCLM and MM5, pointing towards changes in the physical parametrization (i.e. PBL -Planetary Boundary Layer- scheme) as the main factor explaining the differences in the simulations. The correlation patterns between the median wind speed P50 and the mean temperature or the NAO index in ECHAM6 are indeed similar to the ones derived from ECHAM5 and ECHO-G, displaying generally positive, albeit weak, correlations between the median winds and temperature (Fig.3). The correlations between the median wind and the NAO index are positive and strong (Fig.~~3 and Fig.~~5). However, the correlations of these two driving factors with the width of the wind speed distribution, represented by STD, differ in ECHAM6 from the other two versions of ECHAM (Fig.4 and Fig.6). ECHAM6 displays correlation patterns that are positive and spatially more homogeneous, whereas the ECHAM5 and ECHO-G simulations show higher correlations in the Southern Baltic surrounded by negative correlations in Scandinavia and Central Europe. Again, an exception is ECHAM5 correlation between mTemp and STD, which shows an over all negative relationship. Physically, the relationship between mTemp and median wind is positive (but statistically not significant) in the ECHAM6 simulation. This indicates that warmer temperatures are accompanied by a shift towards higher wind speeds and by a slight tendency to a broader wind speed distribution (see also Fig. 4e). tGrad shows negative correlation with the median wind, consistent with the link between a decreased temperature gradient in warmer periods~~(see also Fig. 6e)~~.

4.4 The reanalysis data coastDat2 and NCEP

We present the link between the large-scale drivers and the wind speed distribution for the two reanalysis products NCEP and coastDat2. It can be argued that these two reanalysis data sets should be closer to the real climate, because they both incorporate information based on meteorological observations. On the other hand, the reanalysis models are integrated over a relatively short period of time of about 60 years. Therefore the decadal-scale links between the large-scale climate drivers and the probability distribution of wind speed derived from these data sets is most likely afflicted with a higher degree of uncertainty. The correlation patterns derived from NCEP and coastDat2 are based on gliding 5-year windows, instead of 30-year windows as for the longer simulations described before.

The correlation between mTemp and the parameters of the wind speed distribution for coastDat2 and NCEP shows generally significant positive values with P50, STD, P95 and P99, but no significant

520 correlation for diffM and diffE. The spatially resolved correlation between mTemp and P50 (Fig. 3f+g) and the STD field (Fig. 4f+g) is also dominated by positive values, with highest coefficients over southern Norway, and weaker or slightly negative correlations in the southern regions of the domain(s. Fig. 4f). Therefore, the correlation patterns in the reanalysis data represent a shift of the wind speed distribution from low to high wind speeds during warmer periods, with a tendency to

525 wider wind speed distribution in the northern and a small influence of temperature in the southern regions.

The relationship between tGrad and mTemp is negative (-0.25 for coastDat2, -0.52 for NCEP), again showing that colder periods are related to stronger meridional temperature gradients in agreement with all other models analysed here. Thus, the results obtained from the reanalysis products resem-

530 ble more closely the ones derived from the global climate model simulations (ECHAM5, ECHAM6, ECHO-G) than from the regional simulations (MM5 and CCLM).

The correlation between tGrad and the distribution of wind speed is found to be predominantly weak in the coastDat2 data, with the only statistically significant mentionable value (0.34) for the correlation tGrad-diffM. This result means that higher temperature differences between North and South

535 are slightly correlated with a broader wind speed distribution. In contrast, for the NCEP reanalysis, the link is strong but opposite: weaker meridional gradients are linked to stronger median winds and wider wind speed distributions.

Regarding the link to the NAO, both reanalysis data sets display a consistent picture, with a positive NAO closely linked to stronger median winds and wider distributions (STD) in most of the

540 domain. This link is stronger over the northern regions and becomes smaller and even negative over the southern fringes of the domain. Again, this spatial structure resembles more closely the structure provided by the global models and differs from the pattern provided by the regional models.

4.5 Results in the overlapping time periods 1655-1990 and 1948-1990

This section is dedicated to the comparison of the above explained results with results for the

545 overlapping time periods without (1655-1990 AD, 30y running mean) and with reanalysis data (1948-1990 AD, 5y running mean). Regarding the overlapping period 1655 to 1990 the main conclusions remain the same for both, Table 3 and figures 3-6. In Table 3 some correlations become higher (mTemp), whereas some stay at the same level (NAO, tGrad - beside ECHAM6 which shows now values around zero) and some are lower (mTemp-tGrad). The conclusions concerning the spatial

550 correlation maps are also very comparable: Due to almost the same time period all four results for CCLM in the overlap show almost identical patterns. The GCM results are also very similar between both periods with slightly higher values for the overlapping period. Only MM5 shows a difference above western and central Europe where positive values occur for the overlapping period (1655-1990

AD) and negative or values around zero for the whole period (1001-1990 AD).

555   Regarding the overlapping period 1948 to 1990 the values and patterns change. Nevertheless each
       model simulation still shows different results, and they do not become more similar to the reanalysis
       data (Fig. 7+8). Figure 7 shows the correlation pattern of mTemp and P50 for the period 1948-1990
       which shows more negative (positive) areas for MM5, ECHO-G, ECHAM6, coastDat2 (CCLM,
       ECHAM5) compared to the results of the whole available time periods. The results for NCEP change
560   only marginally. For the correlation between mTemp and STD (Fig. 8) we also see more negative
       (positive) areas for MM5, ECHO-G, coastDat2, NCEP (ECHAM5). CCLM shows a shift from a
       positive region over the Benelux area to Scandinavia. ECHAM6 stays comparable in both periods.
       Note that for all data sets these results are less robust due to the fewer analysed values.

4.6   Centennial-scale evolution of the wind speed variance over the past millennium

565   In the previous sections we analysed the links between large-scale atmospheric drivers and the dis-
       tribution of wind speed at decadal and multidecadal timescales. The time series of the width of the
       wind speed distribution over the past millennium indicate, however, that the slowly changing soil
       boundary conditions may also have a strong influence on the long-term evolution of the variability
       of wind speed in Northern Europe. ~~Fig.~~ Figure 9a shows the time series of the spatially averaged
570   standard deviation of the wind speed distribution at each model grid-cell for the simulation con-
       ducted with the model ECHAM6. The most remarkable feature of the averaged STD is its almost
       continuous increase during the simulated period. ~~It does not show an obvious relationship with the~~
       ~~evolution of the spatially averaged temperature at these long time scales (Fig. ??).~~ This monotonous
       increase is also seen in the corresponding time series calculated with the output of the ECHAM5
575   simulation (not shown), but not in the data of the ECHO-G (based on ECHAM4) simulation (Fig.
       9b). A suggestion about the origin of the increase in the standard deviation of the wind speed distri-
       bution can be obtained by comparing the spatially resolved STD in the last decades versus the initial
       decades in the simulation. ~~Fig.~~ Figure 10a shows the ratio between the spatially resolved standard
       deviations for the periods 1871-1990 AD (P1) and 1001-1091 AD (P2), respectively. The values of
580   this ratio are higher than unity (STD larger at the end of the simulation) over the land areas of central
       Europe, with a maximum at about 25 degrees east. The standard deviation over oceanic grid-cells
       and over Scandinavia does not change significantly between these two periods in the simulations.
       Again, this spatial pattern of increase in the width of the wind speed distribution is also simulated
       by the ECHAM5 simulation (not shown), but not in ECHO-G where the ratio is scattered around 1
585   (not shown).

       The spatial pattern of changes in STD between the beginning and end of the ECHAM6 and ECHAM5
       simulation suggests that the increase in the width of the wind speed distribution may be related
       to surface-boundary processes. This suggestion is supported by the changes in forest cover in the
       course of the last millennium as reconstructed by Pongratz et al. (2008). This reconstruction was

17

590 used to drive the models ECHAM6 and ECHAM5 (see Sect. 2). The difference in tree fraction in
each model grid-cell between the periods 1871-1990 AD (P1) and 1001-1091 AD (P2) is shown in
~~Fig.~~ Figure 10b. The spatial agreement between the reduction in tree fraction and the widening of
the wind speed distribution between the beginning and the end of the millennium is remarkable and
strongly supports the hypothesis that the distribution of wind speed is mainly affected by land-use

595 changes and related changes in surface roughness length. ~~A~~
This is supported by the analysis of a third time period from 1571 to 1690 AD (P3) which also shows
a strong agreement for the STD ratio (P3/P2; Fig. 10c) and the tree fraction difference (P3-P2; Fig.
10d), albeit with less intense values presumably due to the less intense deforestation in period P3.
Hence, we conclude that a less extensive forest cover causes a widening of the wind speed distribu-

600 tion, and vice versa.
This is also visible for the time series in Figure 11a, which shows the temporal evolution of the tree
fraction (black line) and the 30 year running mean STD for ECHAM6 (green line in Fig.9a multiplied
by -1), both lines show a remarkable agreement in the long-term evolution. The simulation with
ECHAM5 shows a comparable evolution for the STD (not shown). The simulation with the model

605 ECHO-G, which was not driven by changes in land use, does not show a long-term increase or
change in the width of the distribution of wind speeds (see green line in Fig.9b), supporting the
strong influence of land cover changes on the distribution of wind speeds.
Therefore, at ~~centennial~~ multi-centennial timescales the correlation between the wind speed distribu-
tion and temperature that was explored in the previous sections, for ECHAM5 and ECHAM6, could

610 have been indirectly caused by land-use changes. At these timescales, anthropogenic deforestation
and mean temperature exhibit a positive trend. Thus the expansion of the wind speed distribution
and the increase of temperature in these decades might be induced by physically different factors,
leading to positive correlations in our analysis. ~~This~~
Figure 11a shows the temporal evolution of the tree fraction used to drive ECHAM5 and ECHAM6

615 (black line). This proves that on shorter time scales (e.g. 100 or 200 years) the effect of this surface-boundary
process is negligible, especially before the 17th century when the trend is very weak. Figures 11b+c
exhibit the correlation between mTemp and the STD for the periods P1 and P2 calculated with a 5
year running mean. Hence, these figures show the relationship between mean temperature and the
wind speed distribution independent of the deforestation effect. Therefore, this statistical effect can

620 be disentangled by separating the analysis of these simulations into two ~~parts (P1~~ time periods (TP1:
years 850-1500 AD, ~~P2~~ TP2: years 1500-2005 AD).
The correlations between mean temperature and the width of the wind distribution does show a
difference in the correlation. For ~~P1~~ TP1 of ECHAM6 mTemp-diffM is around 0 and mTemp-
diffE -0.25, for P2 0.63 and 0.57, respectively. For ~~P1~~ TP1 of ECHAM5 mTemp-diffM is -0.26

625 and mTemp-diffE is -0.38, for ~~P2~~ TP2 0.26 and 0.12, respectively. Both ~~parts~~ time periods in the
GCMs show different signs for the relation between mean temperature and the shape of the wind

18

speed distribution. These results suggest that specifically for ECHAM6 the correlation between the mean temperature and the width of the wind speed distribution is a statistical artifact mediated by deforestation.

630 **5 Discussion and conclusions**

This study investigates and compares different simulation data sets and reanalysis products, on time scales covering the last decades to the past millennium, regarding the probability distribution of the daily wind speed in winter time over Northern Europe. Our investigation is aimed at identifying the large-scale factors that drive changes in this probability distribution. The study is based on corre-

635 lations between different parameters of the wind speed distribution and different climatic indices related to mean temperature, meridional temperature gradient and the North Atlantic Oscillation. The overlaying question is whether and how the wind speed distribution may change during varying climate conditions and hence whether these conditions may provoke more and/or stronger wind speed extremes.

640 One prominent result is that the link between the thermal indices and the North Atlantic Oscillation appears physical consistent in all data sets, and thus all models are consistent in this regard. The relationship between the NAO and mean temperature ~~in wintertime is~~ over Europe is a known effect (Rutgersson et al., 2015), in wintertime this is also positive in all models~~, as this~~. This effect is caused by the advection of maritime air masses by stronger westerly winds in a more positive NAO

645 state (also discussed in Gómez-Navarro et al., 2015a). Also, the correlation between mean Temperature (mTemp) and the temperature gradient (tGrad) shows negative values for all models, indicating that warmer periods are linked to a weakened meridional temperature gradient. This might be explained by the fact that northern regions warm (cool) more strongly when the overall temperature is higher (lower). In climate change projections this is referred to as polar amplification, although

650 it has been also identified in paleoclimate simulations and reconstructions over the past millennium (Luterbacher et al., 2002).

However, a second important result is that the correlation between the large-scale indices and the parameters of the wind speed distribution exhibit markedly different results among the data sets analysed and it is difficult to derive general conclusions on the effect of these large-scale drivers on

655 the distribution of daily wind. Comparable difficulties are reported by Fischer-Bruns et al. (2005). They analysed two simulations of ECHO-G. One simulation showed a link between temperature and storm track variability over the North Atlantic Ocean, which also would have an influence on the wind speed over Europe, whereas the other simulation did not show such a connection. Furthermore, these authors conducted a literature review about climate change experiments with global climate

660 models which lead to different conclusions. Some models therein indicated an intensification of North Atlantic storm tracks, whereas others showed no changes during a warming climate or even a

19

reduction of extreme winds in the North Atlantic area.

Nevertheless, in our study the three global simulations present similarities that warrant to place them in one group. Fig. 3 through 6 show patterns of correlations obtained in the global simulations that are generally similar. This can be expected to a certain degree because the three atmospheric models included in the GCM belong to the same ECHAM family. And further analyses with completely different GCM families would be necessary to reinforce our findings. Likewise, the correlation patterns obtained from the two regional models are also generally similar, although in this case both models, MM5 and CCLM, are structurally different.

The striking result is that the regional models do not seem to inherit the dynamical properties of their respective global models, but produce instead different correlation patterns between the large-scale drivers and the wind speed distributions. In the case of the link between the median wind and the large-scale drivers, the differences between each regional model and its driving global model mostly occur over land areas (see Fig. 3 and 5). However, in case of the link between the standard deviation of wind speed and the large-scale drivers, the differences seem spatially more complex (see Fig. 4 and 6). It is plausible that the higher resolution and the different parametrization schemes of the boundary layer shape the link between the large-scale dynamics and turbulent processes that modulate the width of the daily wind distribution. As Hall (2014) and Gómez-Navarro et al. (2013) already stated the RCMs should provide a better representation of small-scale processes, topographic influences and of the land-sea contrasts, and thus should be better suited for the simulation of extreme events.

The comparison of the correlation coefficients in Table 3 shows differences in signs and statistical significance. Regarding statistical significance, it is noticeable that for tGrad and wind speed there are only significant values for MM5 and NCEP, although with different signs. CCLM as one of the regional model simulations is the only simulation which shows almost no significant correlations. Its forcing global model ECHAM5 only shows significance for the NAO - wind speed correlation. ECHAM6 as the successor of ECHAM5 also shows only significant values for tGrad - mTemp and for NAO - wind. ECHO-G and coastDat2 show significant values only for wind speed values in correlation with mTemp and NAO.

The correlation between tGrad and wind speed shows significant values only for MM5 and NCEP but both data sets exhibit different signs. MM5 reveals positive correlations, which implies that stronger winds are associated with a stronger temperature gradient. This positive correlation is only appreciated for the regional data sets: MM5, CCLM and coastDat2. The global data sets, ECHO-G, ECHAM5, ECHAM6 and NCEP, show negative values, indicating stronger winds corresponding to weaker temperature gradients. Thus, only the regional data sets support the findings of Li and Woollings (2014), which say that weaker meridional temperature gradients induce weaker or less storms due to a weaker baroclinicity. These results demonstrate that the influence of the spatial resolution and especially the different boundary layer parametrization may be a critical factor to establish a link between climate change and changes in near-surface wind speeds.

20

Another indicator for the influence of the spatial resolution on our results might be the fact that only the regional simulations MM5 and CCLM show strong negative correlations between mean temperature and the width of the probability distribution as measured by diffM/diffE. These correlations suggest that colder periods are connected with stronger wind speed extremes. In contrast, the GCM data show no clear correlations between these parameters. This study does not allow us to provide a comprehensive dynamical explanation for the different behavior of wind speeds in changing temperature or pressure conditions: the models show different results although each model seems to be dynamical consistent in itself. Therefore, a detailed analysis of each of the simulations, and maybe of the computer codes, ~~seems required~~ becomes necessary to understand how the different correlation patterns arise.

On centennial timescales, we identified land-use changes as a very important factor modulating near-surface wind in the simulations. Note that anthropogenic changes in land-use are prescribed only in the ECHAM5 and ECHAM6 simulations, whereas for ECHO-G land-use is kept constant during the whole simulation. The analysis of the ECHAM5 and ECHAM6 millennium simulations reveals a strong increase of the standard deviation of wind speed for the last decades since the industrialization, and in areas that coincide with larger deforestation along the last centuries. The impact of land-use changes on wind conditions was also shown by Pessacg and Solman (2013) in simulations with the regional model MM5 over South America for different idealized land-use scenarios.

The main conclusion that can be drawn from this study is that the link between large-scale climate drivers and the distribution of daily wind speeds in wintertime in this region is complex and not fully constrained by currently available simulations. All models analysed here have been individually profusely used in climate simulations and the data sets have been used in a number of other previous studies, and no gross deficiencies have been pointed out so far. Our study is ~~different because of the long~~ new because it employs recently available long high-resolution paleo-simulation ~~(e.g. MM5, which is rather used as a short time prediction model), and the comparison of~~, and compares all these models regarding a relationship between temperature and NAO conditions and wind speed. We conclude that, although climate models may be dynamically sound in the large-scale contest, the impact of climate change on variables like near-surface wind speed distribution possibly depends more strongly on the details of the physical parametrization and changes in surface forcing, like deforestation, than on the large-scale dynamical drivers, such as large-scale temperature or sea-level-pressure changes.

21

References

735

2k Consortium, P. (2013). Continental-scale temperature variability during the past two millennia. *Nature Geoscience*, 6:339–346.

Bard, E., Raisbeck, G., Yiou, F., and J., J. (2000). Solar irradiance during the last 1200 years based on cosmogenic nuclides. *Tellus*, 52B:985–992.

740 Bretagnon, P. and Francou, G. (1988). Planetary theories in rectangular and spherical variables – vsop87 solutions. *Astron. Astrophys.*, 202:309–315.

Brönnimann, S., Martius, O., von Waldow, H., Welker, C., Luterbacher, J., Compo, G., Sardeshmukh, P., and Usbeck, T. (2012). Extreme winds at northern mid-latitudes since 1871. *Meteor. Z.*, 21(1):013–027.

Cattiaux, J. and Cassou, C. (2013). Opposite cmip3/cmip5 trends in the wintertime northern annular mode
745 explained by combined local sea ice and remote tropical influences. *Geophys. Res. Lett.*, 40:3682–3687.

Compo, G. P., Whitaker, J. S., Sardeshmukh, P. D., Matsui, N., Allan, R. J., Yin, X., Gleason, B. E., Vose, R. S., Rutledge, G., Bessemoulin, P., Brönnimann, S., Brunet, M., Crouthamel, R. I., Grant, A. N., Groisman, P. Y., Jones, P. D., Kruk, M. C., Kruger, A. C., Marshall, G. J., Maugeri, M., Mok, H. Y., Nordli, O., Ross, T. F., Trigo, R. M., Wang, X. L., Woodruff, S. D., and Worley, S. J. (2011). The twentieth century reanalysis
750 project. *Quarterly Journal of the Royal Meteorological Society*, 137(654):1–28.

Costas, I. (2013). *Climate Archive Dune*. PhD thesis, Hamburg University.

Crowley, T. J., Zielinski, G., Vinther, B., Udisti, R., Kreutz, K., Cole-Dai, J., and Castellano, J. (2008). Volcanism and the little ice age. *PAGES Newsletter*, 16:22–23.

Crueger, T., Stevens, B., and Brokopf, R. (2013). The madden–julian oscillation in echam6 and the introduction
755 of an objective mjo metric. *J. Climate*, 26:3241–3257.

Doms, G., J. F., Heise, E., Herzog, H.-J., Mrionow, D., Raschendorfer, M., Reinhart, T., Ritter, B., Schrodin, R., Schulz, J.-P., and Vogel, G. (2011). A description of the nonhydrostatic regional cosmo model. part ii: Physical parameterization. Technical report, Deutscher Wetterdienst.

Donnelly, J. P. and Woodruff, J. D. (2007). Intense hurricane activity over the past 5,000 years controlled by el
760 niño and the west african monsoon. *Nature*, 447:465–468.

Ebisuzaki, W. (1997). A method to estimate the statistical significance of a correlation when the data are serially correlated. *J. Climate*, 10:2147–2153.

Esper, J., Düthorn, E., Krusic, P., Timonen, M., and Büntgen, U. (2014). Northern european summer temperature variations over the common era from integrated tree-ring density records. *Journal of Quaternary*
765 *Science*, 29:487–494.

Etheridge, D., Steele, L., Langenfelds, R., Francey, R., Barnola, J., and Morgan, V. (1996). Natural and anthropogenic changes in atmospheric co2 over the last 1000 years from air in antarctic ice and firn. *J. Geophys. Res.*, 101:4115–4128.

Fernandez-Donado, L., Gonzalez-Rouco, J. F., Raible, C. C., Ammann, C. M., Barriopedro, D., Garcia-
770 Bustamante, E., Jungclaus, J. H., Lorenz, S. J., Luterbacher, J., Phipps, S. J., Servonnat, J., Swingedouw, D., Tett, S. F. B., Wagner, S., Yiou, P., and Zorita, E. (2013). Large-scale temperature response to external forcing in simulations and reconstructions of the last millennium. *Clim. Past*, 9:393–421.

Feser, F., Barcikowska, M., Krueger, O., Schenk, F., Weisse, R., and Xia, L. (2015). Storminess over the north atlantic and northwestern europe—a review. *Q.J.R. Meteorol. Soc.*, 141:350–382.

22

775   Feser, F., Rockel, B., von Storch, H., Winterfeldt, J., and Zahn, M. (2011). Regional climate models add value to global model data: A review and selected examples. *Bull. Amer. Meteor. Soc.*, 92(9):1181–1192.

Fischer-Bruns, I., von Storch, H., Gonzalez-Rouco, J. F., and Zorita, E. (2005). Modelling the variability of midlatitude storm activity on decadal to century time scales. *Climate Dyn.*, 25:461–476.

Geyer, B. (2014). High resolution atmospheric reconstruction for europe 1948–2012: coastdat2. *Earth Syst.*
780   *Sci. Data.*, 6:147–164.

Gillett, N. P. and Fyfe, J. C. (2013). Annular mode changes in the cmip5 simulations. *Geophys. Res. Lett.*, 40:1189–1193.

Giorgetta, M. A., Jungclaus, J., Reick, C. H., Legutke, S., Bader, J., Böttinger, M., Brovkin, V., Crueger, T., Esch, M., Fieg, K., Glushak, K., Gayler, V., Haak, H., Hollweg, H.-D., Ilyina, T., Kinne, S., Kornblueh, L.,
785   Matei, D., Mauritsen, T., Mikolajewicz, U., Mueller, W., Notz, D., Pithan, F., Raddatz, T., Rast, S., Redler, R., Roeckner, E., Schmidt, H., Schnur, R., Segschneider, J., Six, K. D., Stockhause, M., Timmreck, C., Wegner, J., Widmann, H., Wieners, K.-H., Claussen, M., Marotzke, J., and Stevens, B. (2013). Climate and carbon cycle changes from 1850 to 2100 in mpi-esm simulations for the coupled model intercomparison project phase 5. *J. Adv. Model. Earth Syst.*, 5:572–597.

790   Gómez-Navarro, J. J., Bothe, O., Wagner, S., Zorita, E., Werner, J. P., Luterbacher, J., Raible, C. C., and Montávez, J. P. (2015a). A regional climate palaeosimulation for europe in the period 1501–1990 – part ii: Comparison with gridded reconstructions. *Clim. Past Discuss.*, 11:307–343.

Gómez-Navarro, J. J., Montávez, J. P., Wagner, S., and Zorita, E. (2013). A regional climate palaeosimulation for europe in the period 1500–1990 – part 1: Model validation. *Clim. Past*, 9:1667–1682.

795   Gómez-Navarro, J. J., Raible, C. C., and Dierer, S. (2015b). Sensitivity of the wrf model to pbl parametrizations and nesting techniques: evaluation of surface wind over complex terrain. *Geosci. Model Dev. Discuss*, 8:5437–5479.

Gómez-Navarro, J. J. and Zorita, E. (2013). Atmospheric annular modes in simulation over the past millennium: No long-term response to external forcing. *Geophys. Res. Lett.*, 40:3232–3236.

800   Hall, A. (2014). Projecting regional change. *Science*, 346:1461.

Hall, A. and Qu, X. (2006). Using the current seasonal cycle to constrain snow albedo feedback in future climate change. *Geophys. Res. Lett.*, 33:L03502.

Hong, S.-Y. and Pan, H.-L. (1996). Nonlocal boundary layer vertical diffusion in a medium-range forecast model. *Mon. Wea. Rev.*, 124:2322–2339.

805   Hunt, B. (2006). The medieval warm period, the little ice age and simulated climatic variability. *Climate Dynamics*, 27(7-8):677–694.

Hünicke, B., Zorita, E., and Haeseler, S. (2011). Holocene climate simulations for the baltic sea region - application for sea level and verification of proxy data. *Berichte der RGK*, 92:211–249.

Jungclaus, J. H., Lorenz, S. J., Timmreck, C., Reick, C. H., Brovkin, V., Six, K., Segschneider, J., Giorgetta,
810   M. A., Crowley, T. J., Pongratz, J., Krivova, N. A., Vieira, L. E., Solanki, S. K., Klocke, D., Botzet, M., Esch, M., Gayler, V., Haak, H., Raddatz, T. J., Roeckner, E., Schnur, R., Widmann, H., Claussen, M., Stevens, B., and Marotzke, J. (2010). Climate and carbon-cycle variability over the last millennium. *Clim. Past*, 6:723–737.

Kalnay, E. and Coauthors (1996). The ncep/ncar 40-year reanalysis project. *Bull Am Meteorol Soc*, 77:437–471.

815   Kistler, R. and Coauthors (2001). The ncep/ncar 50-year reanalysis: Monthly means cd–rom and documenta-
tion. *Bull Am Meteorol Soc*, 82:247–267.

Krivova, N. and Solanki, S. (2008). Models of solar irradiance variations: Current status. *Journal of Astro-
physics and Astronomy*, 29(1-2):151–158.

Krueger, O., Schenk, F., Feser, F., and Weisse, R. (2013). Inconsistencies between long-term trends in stormi-
820   ness derived from the 20cr reanalysis and observations. *J. Climate*, 26:868–874.

Legutke, S. and Voss, R. (1999). The hamburg atmosphere –ocean coupled circulation model echo-g. Technical
Report 18, DKRZ, Hamburg.

Li, M. and Woollings, T. (2014). Extratropical cyclones in a warmer, moister climate: A recent atlantic analogue.
Geophys. Res. Lett., 41(23):8594–8601.

825   Luterbacher, J., Dietrich, D., Xoplaki, E., Grosjean, M., and Wanner, H. (2004). European seasonal and annual
temperature variability, trends, and extremes since 1500. *Science*, 303:1499–1503.

Luterbacher, J., Xoplaki, E., Dietrich, D., Rickli, R., Jacobeit, J., Beck, C., Gyalistras, D., Schmutz, C., and
Wanner, H. (2002). Reconstruction of sea level pressure fields over the eastern north atlantic and europe
back to 1500. *Climate Dynamics*, 18(7):545–561.

830   Marland, G., Boden, T., and Andres, R. (2003). Global, regional, and national emissions, trends: a compendium
of data on global change. Technical report, Carbon Dioxide Information Center, Oak Ridge National Labo-
ratory, US Department of Energy, Oak Ridge, TN.

Marsland, S. J., Haak, H., Jungclaus, J. H., Latif, M., and Roeske, F. (2003). The max planck institute global
ocean/sea ice model with orthogonal curvilinear coordinates. *Ocean Modell*, 5:91–127.

835   Pessacg, N. L. and Solman, S. (2013). Effects of land-use changes on climate in southern south america.
Climate Research, 55(1):33–51.

Pithan, F. and Mauritsen, T. (2014). Arctic amplification dominated by temperature feedbacks in contemporary
climate models. *Nature Geosci*, 7:181–184.

Pongratz, J., Reick, C., Raddatz, T., and Claussen, M. (2008). A reconstruction of global agricultural areas and
840   land cover for the last millennium. *Global Biogeochem. Cycles,*, 22:GB3018.

Rockel, B. W. and Hense, A. (2008). The regional climate model cosmo-clm (cclm). *Meteorol. Z.*, 12:347–348.

Roeckner, E., Arpe, K., Bengtsson, L., Christoph, M., Claussen, M., Dümenil, L., Esch, M., Giorgetta, M.,
Schlese, U., and Schulzweida, U. (1996). The atmospheric general circulation model echam4: model de-
scription and simulation of present-day climate. Technical Report 218, MPI-M, Hamburg.

845   Roeckner, E., Bäuml, G., Bonaventura, L., Brokopf, R., Esch, M., Giorgetta, M., Hagemann, S., Kirchner,
I., Kornblueh, L. ., Manzini, E., Rhodin, A., Schlese, U., Schulzweida, U., and Tompkins, A. (2003). The
atmospheric general circulation model echam5. part i: Model description. Technical Report 349, Max Planck
Institute for Meteorology, Hamburg.

Rutgersson, A., Jaagus, J., Schenk, F., Stendel, M., Bärring, L., Briede, A., Claremar, B., Hanssen-Bauer, I.,
850   Holopainen, J., Moberg, A., Nordli, O., Rimkus, E., and Wibig, J. (2015). *Recent Change—Atmosphere*,
chapter Second Assessment of Climate Change for the Baltic Sea Basin, pages 69–97. Springer International
Publishing.

Schimanke, S., Meier, H. E. M., Kjellström, E., Strandberg, G., and Hordoir, R. (2012). The climate in the baltic
sea region during the last millennium simulated with a regional climate model. *Clim. Past*, 8:1419–1433.

855   Schmidt, G., Jungclaus, J.H. andAmmann, C., Bard, E., Braconnot, P., Crowley, T., Delaygue, G., Joos, F.,
      Krivova, N., Muscheler, R., Otto-Bliesner, B., Pongratz, J., Shindell, D., Solanki, S., Steinhilber, F., and
      Vieira, L. (2011). Climate forcing reconstructions for use in pmip simulations of the last millennium (v1.0).
      Geosci. Model Dev., 4:33–45.

      Schreiber, T. and Schmitz, A. (1996). Improved surrogate data for nonlinearity tests. *Phys. Rev. Lett.*, 77:635.

860   Seneviratne, S., Nicholls, N., Easterling, D., Goodess, C., Kanae, S., Kossin, J., Luo, Y., Marengo, J., McInnes,
      K., Rahimi, M., Reichstein, M., Sorteberg, A., Vera, C., and Zhang, X. (2012). Changes in climate extremes
      and their impacts on the natural physical environment. in: Managing the risks of extreme events and disasters
      to advance climate change adaptation [field, c.b., v. barros, t.f. stocker, d. qin, d.j. dokken, k.l. ebi, m.d.
      mastrandrea, k.j. mach, g.-k. plattner, s.k. allen, m. tignor, and p.m. midgley (eds.)]. a special report of
865   working groups i and ii of the intergovernmental panel on climate change (ipcc). Technical report, Cambridge
      University Press, Cambridge, UK, and New York, NY, USA.

      Stevens, B., Giorgetta, M., Esch, M., Mauritsen, T., Crueger, T., Rast, S., M., S., Schmidt, H., Bader, J., Block,
      K., Brokopf, R., Fast, I., Kinne, S., Kornblueh, L., Lohmann, U., Pincus, R., Reichler, T., and Roeckner, E.
      (2013). Atmospheric component of the mpi-m earth system model: Echam6. *J. Adv. Model. Earth Syst*,
870   5:146–172.

      Taylor, K. E., Stouffer, R. J., and Meehl, G. A. (2012). An overview of cmip5 and the experiment design. *Bull.
      Amer. Meteor. Soc.*, 93:485–498.

      von Storch, H., Langenberg, H., and Feser, F. (2000). A spectral nudging technique for dynamical downscaling
      purposes. *Mon. Weather Rev.*, 128:3664 – 3673.

875   von Storch, H., Zorita, E., Jones, J., Dimitriev, Y., González-Rouco, F., and Tett, S. (2004). Reconstructing past
      climate from noisy data. *Science*, 306:679–682.

      Wang, X., Wan, H., Zwiers, F., Swail, V., Compo, G., Allan, R., Vose, R., Jourdain, S., and X., Y. (2011). Trends
      and low-frequency variability of storminess over western europe, 1878-2007. *Climate Dyn.*, 37:2355–2371.

      Wang, X. L., Feng, Y., Compo, G. P., Zwiers, F. W., Allan, R. J., Swail, V. R., and Sardeshmukh, R. D. (2013).
880   Is the storminess in the twentieth century reanalysis really inconsistent with observations? a reply to the
      comment by krueger et al. (2013b). *Clim. Dyn.*, 42:1113–1125.

      Wolff, J., Maier-Reimer, E., and Legutke, S. (1997). The hamburg primitive equation model hope. Technical
      Report 8, Germany Climate Computer Center (DKRZ), Hamburg.

      Yin, J. H. (2005). A consistent poleward shift of the storm tracks in simulations of 21st century climate.
885   *Geophysical research letters*, 32(18):L18701.

      Zorita, E., von Storch, H., Gonzalez-Rouco, J. F., Cubasch, U., Luterbacher, J., Legutke, S., Fischer-Bruns, I.,
      and Schlese, U. (2004). Climate evolution in the last five centuries simulated by an atmosphere-ocean model:
      global temperatures, the north atlantic oscillation and the late maunder minimum. *Meteorol. Z*, 13:271–289.
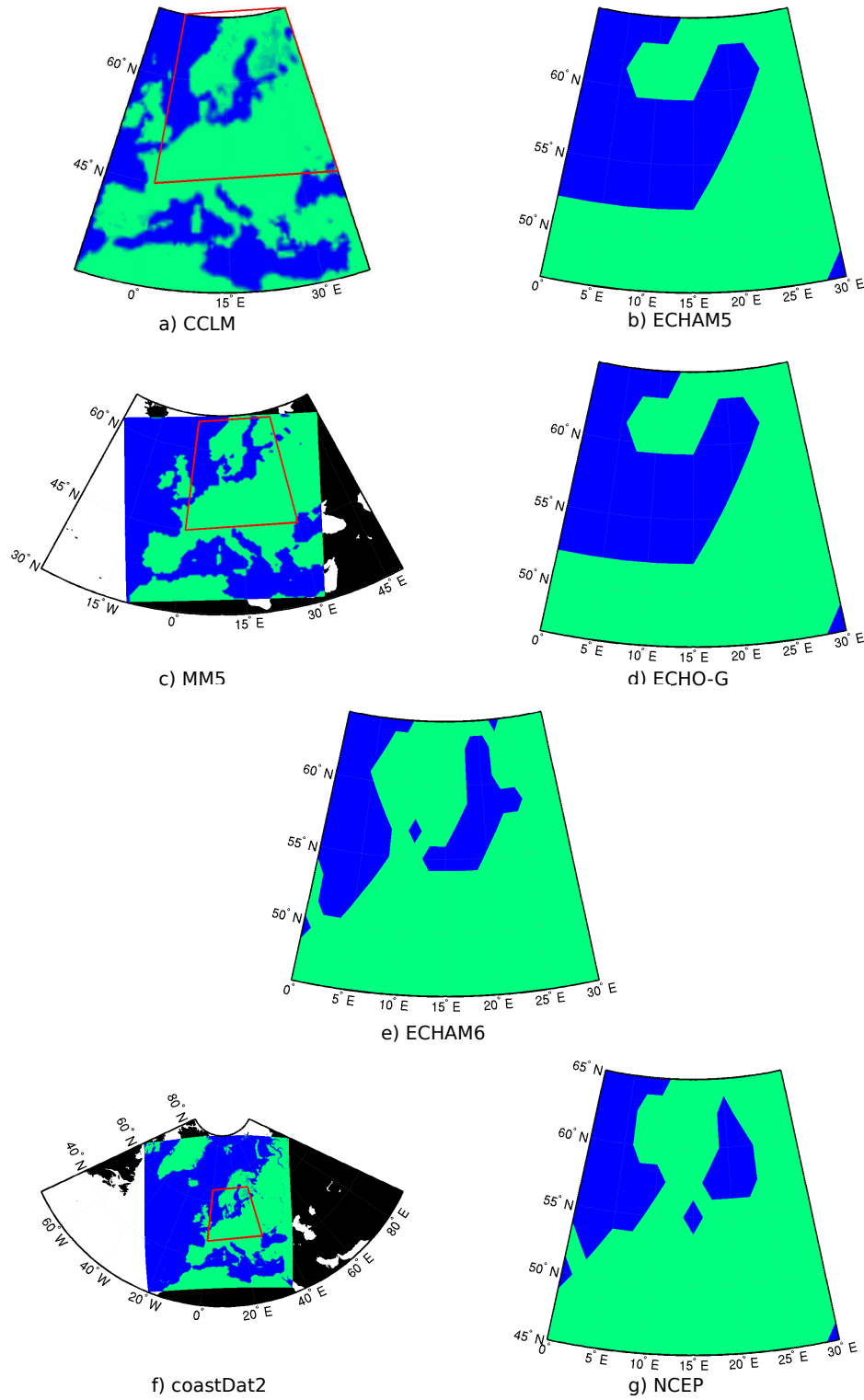
Figure 1: ~~Field correlation of mean Temperature and 50th percentile~~ Land-Sea-Masks of ~~wind speed for 7 different~~ the analysed simulations. Figures regarding global data sets ~~: a) CCLM (1655-1999 AD), b)~~ ECHAM5~~(850-2005 AD), c) MM5 (1001-1990 AD), d) ECHO-G (1001-1990 AD)~~ECHOG, ~~e)~~ ECHAM6~~(850-2005 AD), f~~NCEP~~)~~ ~~coastDat2~~ only show the investigation area. Figures concerning regional data sets ~~(1948-2012 AD)~~CCLM, ~~g) NCEP (1948-2012 AD~~MM5, coastDat2) include the Land-Sea-Mask for the whole simulation domain and the investigation area is shown with a red triangle.

26

expl. Variance: 45.26 %
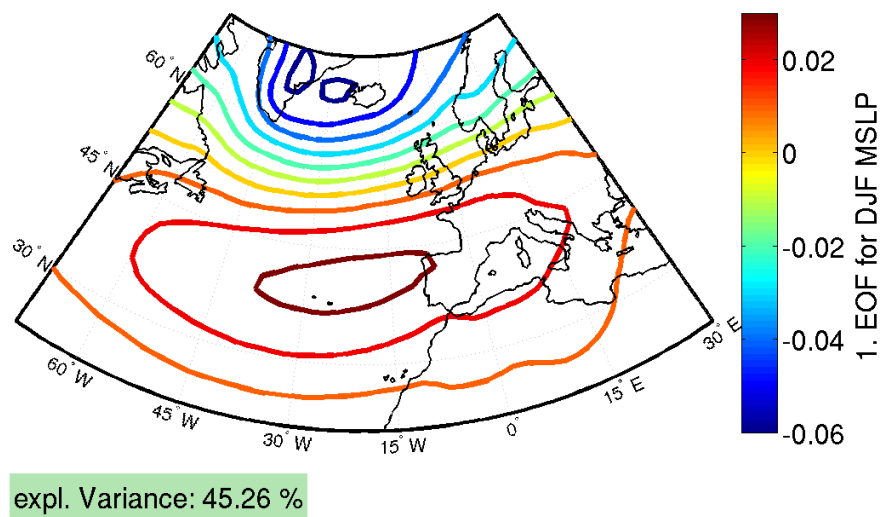
Figure 2: The NAO pattern exemplarily shown for ECHAM6 as the 1. EOF of mean-sea-level-pressure (MSLP). The corresponding principal components are used as the NAO index.
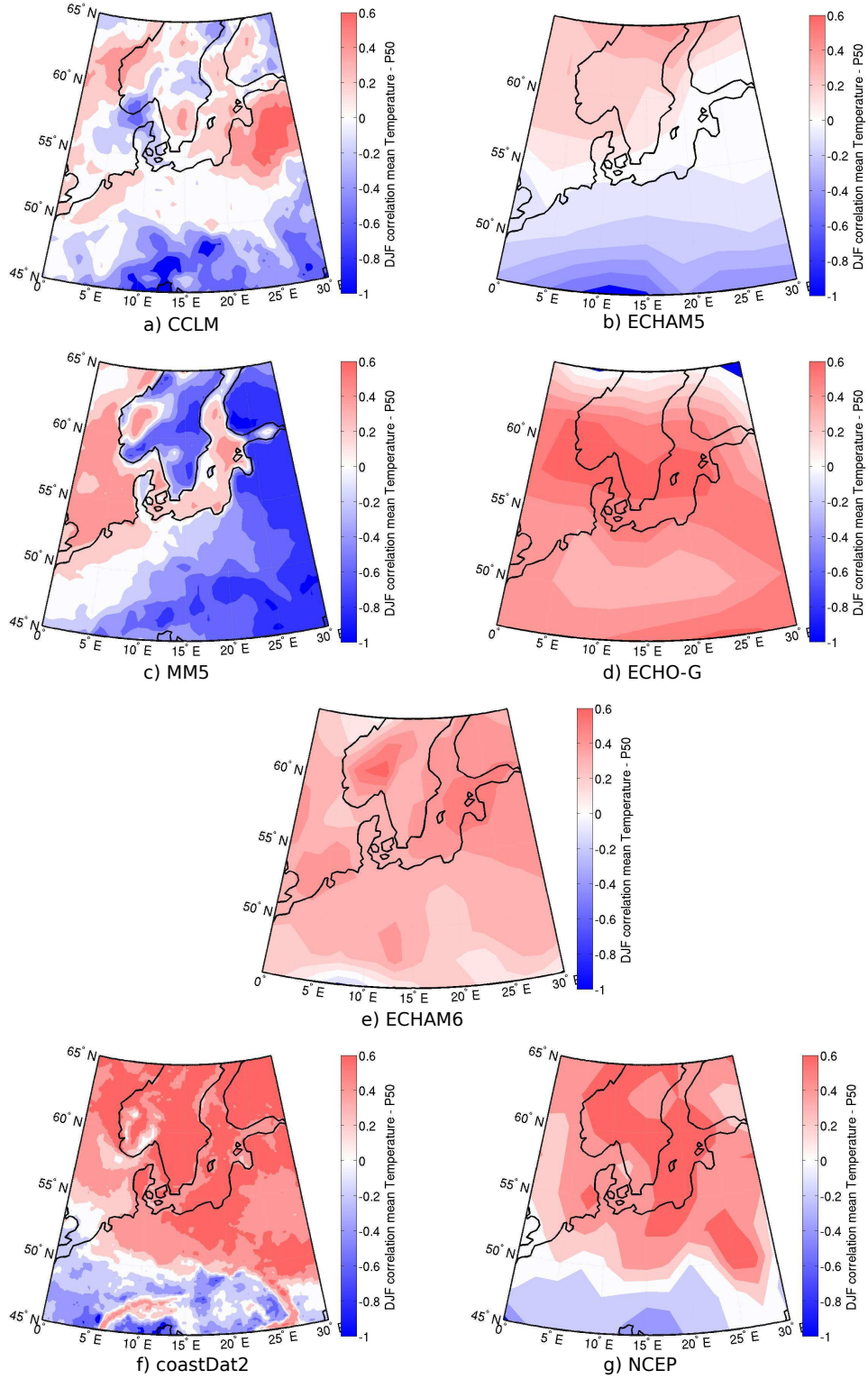
Figure 3: Correlation of field mean Temperature and 50th percentile of wind speed for 7 different data sets: a) CCLM (1655-1999 AD), b) ECHAM5 (850-2005 AD), c) MM5 (1001-1990 AD), d) ECHO-G (1001-1990 AD), e) ECHAM6 (850-2005 AD), f) coastDat2 (1948-2012 AD), g) NCEP (1948-2012 AD)
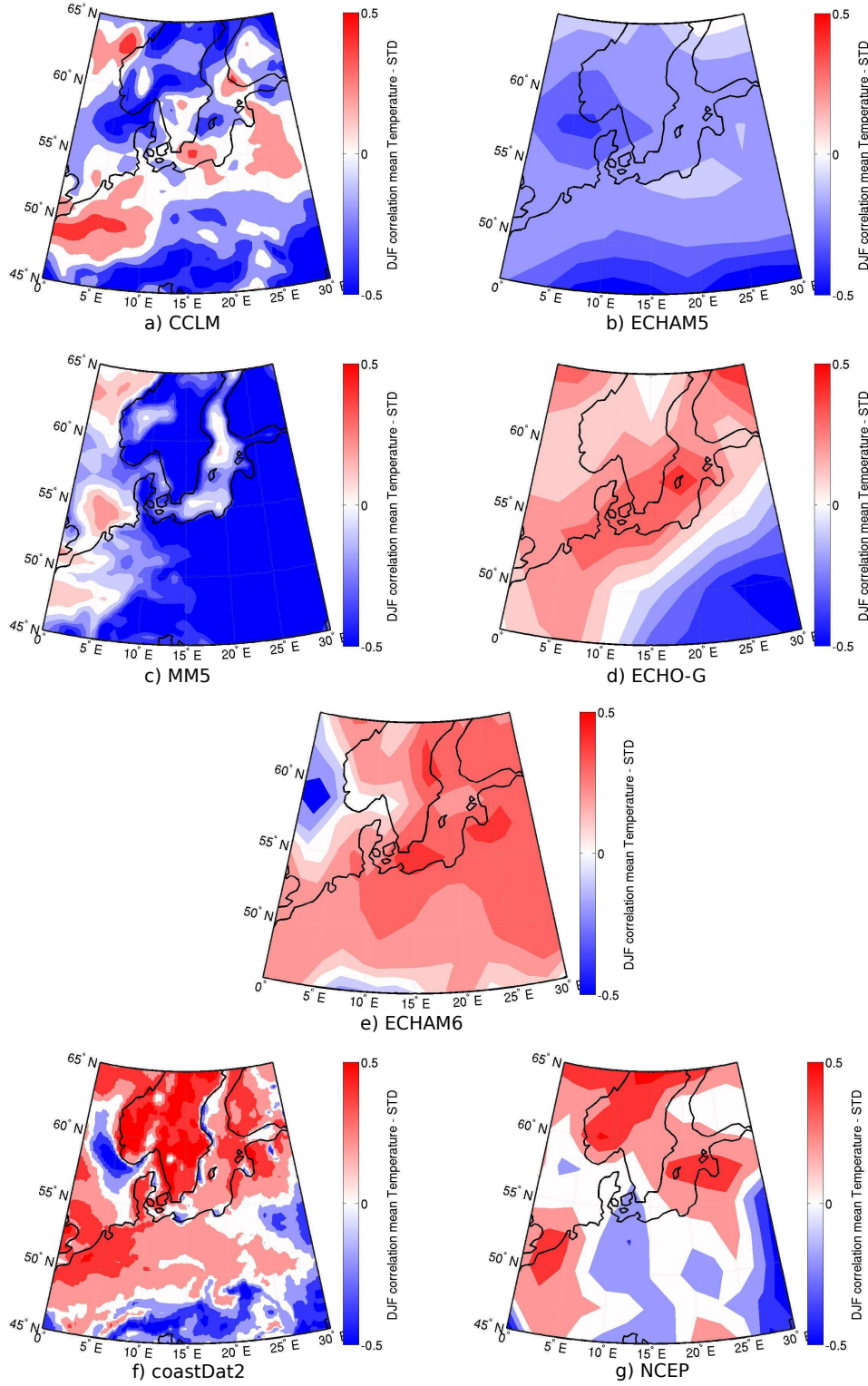
28

Figure 4: ~~Field correlation~~ Correlation between field mean temperature and standard deviation of wind speed for 7 different data sets: a) CCLM (1655-1999 AD), b) ECHAM5 (850-2005 AD), c) MM5 (1001-1990 AD), d) ECHO-G (1001-1990 AD), e) ECHAM6 (850-2005 AD), f) coastDat2 (1948-2012 AD), g) NCEP (1948-2012 AD)
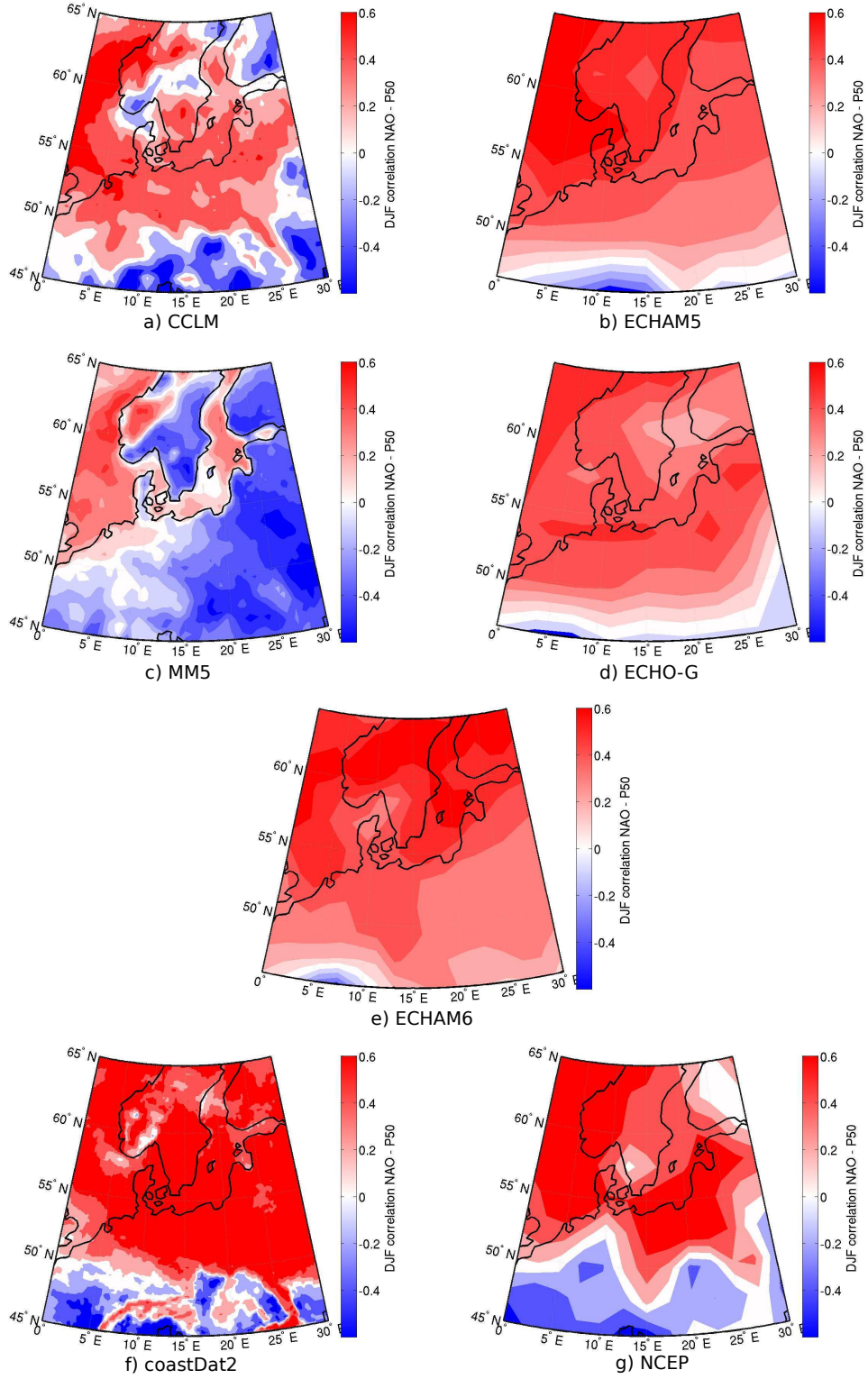
29

Figure 5: ~~Field correlation~~ Correlation between NAO index and 50th percentile of wind speed for 7 different data sets: a) CCLM (1655-1999 AD), b) ECHAM5 (850-2005 AD), c) MM5 (1001-1990 AD), d) ECHO-G (1001-1990 AD), e) ECHAM6 (850-2005 AD), f) coastDat2 (1948-2012 AD), g) NCEP (1948-2012 AD)

30

Figure 6: ~~Field correlation~~ Correlation between NAO index and standard deviation of wind speed for 7 different data sets: a) CCLM (1655-1999 AD), b) ECHAM5 (850-2005 AD), c) MM5 (1001-1990 AD), d) ECHO-G (1001-1990 AD), e) ECHAM6 (850-2005 AD), f) coastDat2 (1948-2012 AD), g) NCEP (1948-2012 AD)
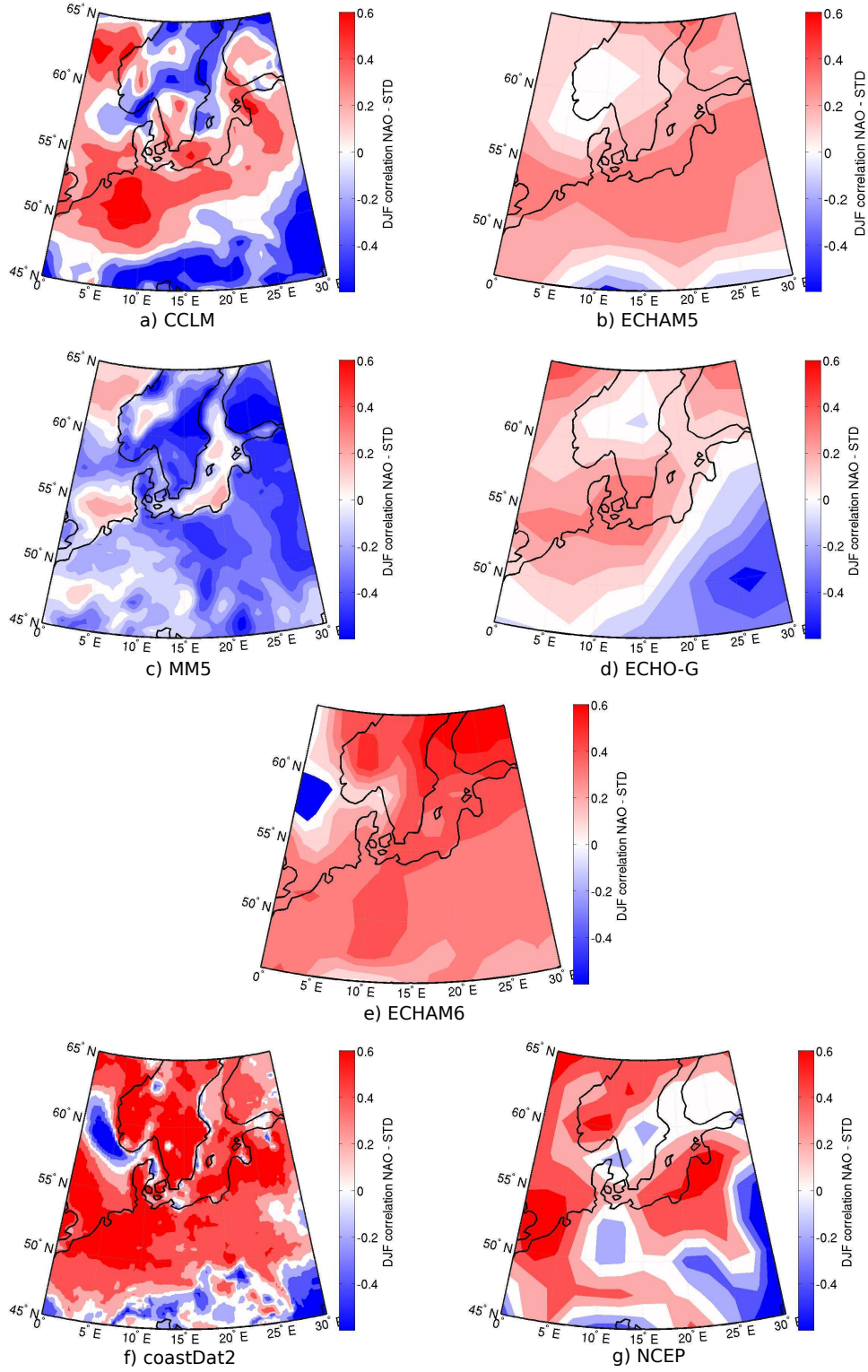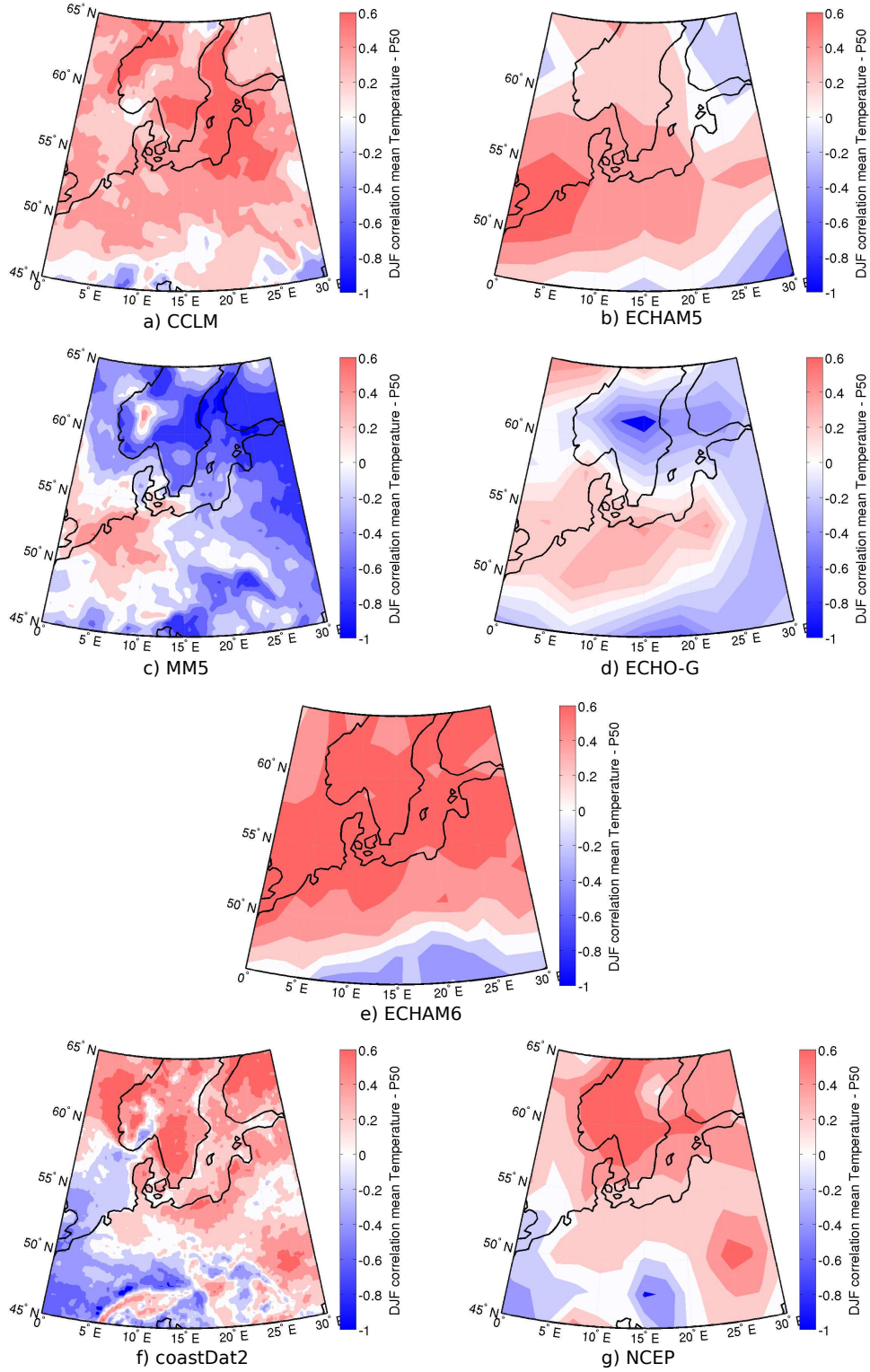
31

Figure 7: ~~Comparison~~ Correlation of ~~yearly~~ field mean ~~temperature~~ Temperature and 50th percentile of wind speed for ~~ECHAM6 (blue~~7 different data sets in the overlapping time period from 1948 to 1990: a) CCLM, b) ECHAM5~~(green~~, c) MM5, d) ~~and~~ ECHO-G~~(red~~, e) ECHAM6, f) coastDat2, g) NCEP

32

Figure 8: ~~Time series~~ Correlation of ~~yearly~~ field mean ~~temperature (blue)~~ Temperature and ~~the standard deviation~~ (STD ~~)~~ of ~~the~~ wind speed ~~(green)~~ for 7 different data sets in the ~~GCMs ECHAM6 (~~overlapping time period from 1948 to 1990: a) ~~and ECHO-G (~~CCLM, b) ~~. In both models the correlation between the blue and the green line is 0.34.~~ECHAM5, c) MM5, d) ECHO-G, e) ECHAM6, f) coastDat2, g) NCEP
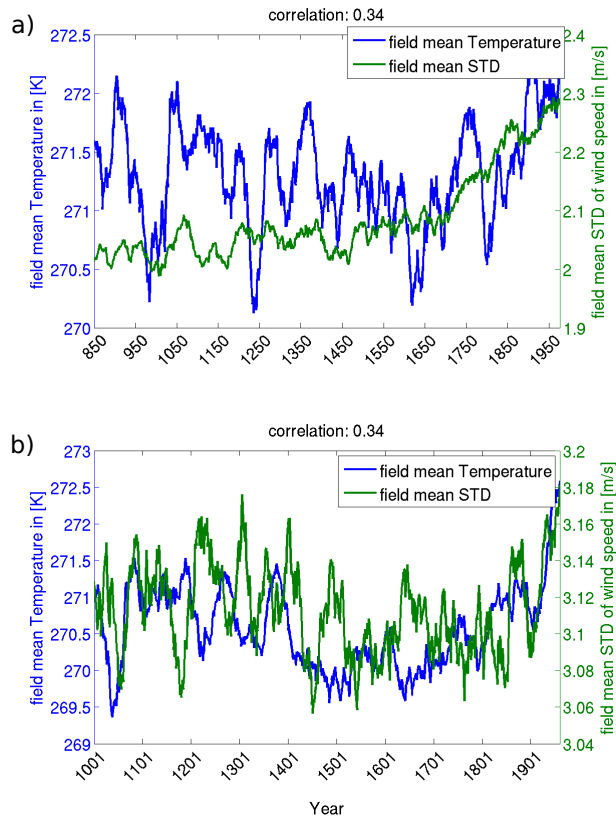
33

Figure 9: Time series of 30 year running mean values of mean temperature (blue) and the standard deviation (STD) of the wind speed (green) for the GCMs ECHAM6 (a) and ECHO-G (b). In both models the correlation between the blue and the green line is 0.34.
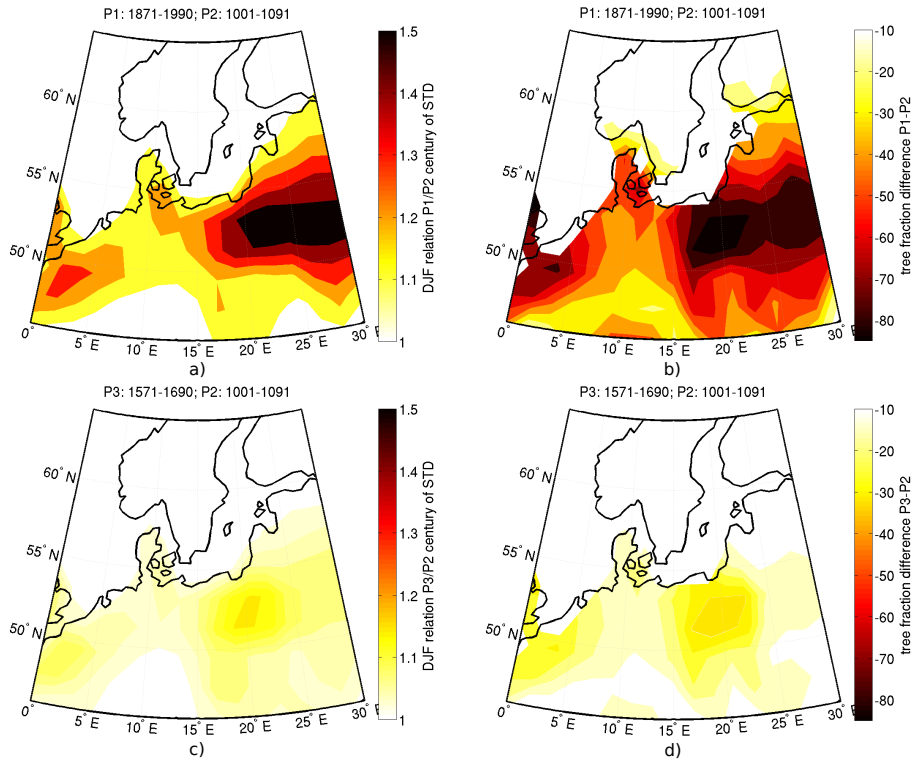
Figure 10: a) Relation between part 1 (P1: 1871-1990 AD) and part 2 (P2: 1001-1091 AD) standard deviation (STD) of wind speed (ECHAM6). b) Tree fraction difference of P1 minus P2 derived from Pongratz et al. (2008). c) Relation between part 3 (P3: 1581-1690 AD) and P2 STD for ECHAM6. d) Tree fraction difference of P3 minus P2 derived from Pongratz et al. (2008).
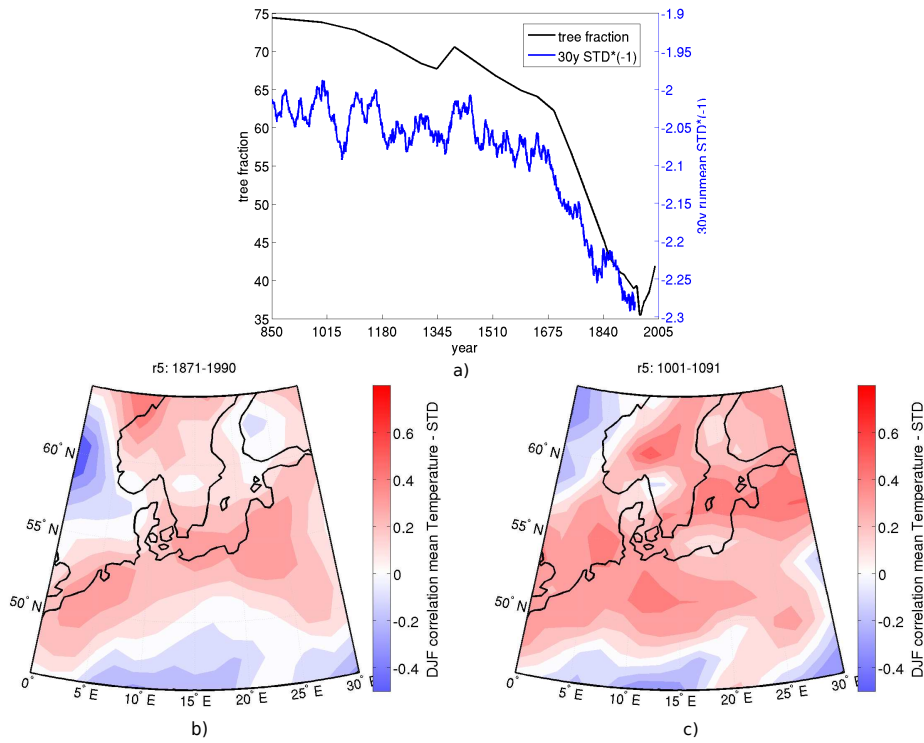
Figure 11: a) tree fraction after Pongratz et al. (2008) (black) averaged over the investigation area. ECHAM6 30 year running mean STD of wind speed (multiplied by -1) (blue). b) correlation between field mean temperature and STD for 1871-1990 with a 5 year running mean computation c) correlation between field mean temperature and STD for 1001-1091 with a 5 year running mean computation.

[t]

Table 1: Overview of the analysed simulations/reanalysis and their simulation acronyms, underlying atmosphere and ocean models, boundary forcings (only for regional data sets) as well as the spatial resolution of the atmosphere models and time periods, as used for the analysis.

	Simulation	Atmosphere	Ocean	Boundary	atm. spatial res.	Vegetation	Period
GCM	ECHO-G	ECHAM4	HOPE-G		3.75°	constant	1001-1990
	ECHAM5	ECHAM5	MPI-OM		3.75°	time dependent	850-2005
	ECHAM6	ECHAM6	MPI-OM		3.75°	time dependent	850-2005
RCM	MM5	MM5		ECHO-G	0.5°	constant	1001-1990
	CCLM	CCLM		ECHAM5	0.5°	constant	1655-1999
Reanalysis	coastDat2	CCLM*		NCEP	0.22°	constant	1948-2012
	NCEP				2.5°	constant	1948-2012

* with spectral nudging

[t]

Table 2: Overview of the GCM forcings. The forcings are abbreviated as follows: S – strong solar forcing (>0.2% change since LMM); s – weak solar forcing (<0.1% change since LMM); G – greehouse gas; V – volcanic; O – orbital; L – land-use change. The last column gives the references describing the experiments.

GCM	Forcings	Reference
ECHO-G	SGV	Zorita et al. (2004)
ECHAM5	SGVOL	Jungclaus et al. (2010)
ECHAM6	sGVOL	Schmidt et al. (2011)

[t]

Table 3: Time correlation coefficients between the following parameters of the probability distribution of daily mean wind speed: standard deviation of wind speed (STD), the 50th, 95th and 99th percentile (P50, P95, P99) and the differences between P95-P50 (diffM) and P99-P95 (diffE) and some large-scale drivers: spatially averaged December-February air temperature (mTemp), the spatial air temperature gradient (tGrad) and the North Atlantic Oscillation index (NAO). The parameters of the probability distributions have been computed in 30 year sliding windows for the simulations and in 5 year sliding windows for the reanalysis products. The time series of the drivers have been smoothed with a running mean filter. Significant ($p < 0.05$) coefficients (tested with a random phased bootstrap method) are written in bold.

	MM5	CCLM	ECHO-G	ECHAM5	ECHAM6	coastDat2	NCEP
tGrad – mTemp	**-0.47**	-0.56	**-0.35**	-0.24 **-0.47**	**-0.53**	-0.25	**-0.52**
tGrad – NAO	**-0.60**	-0.23	**-0.40**	**-0.53**	**-0.70**	-0.31	**-0.54**
NAO – mTemp	**0.66**	**0.72**	**0.72**	**0.57**	**0.68**	**0.79**	**0.79**
mTemp – STD	**-0.76**	-0.26	0.34	0.22 -0.19	0.34	**0.40**	**0.36**
mTemp – P50	**-0.40**	0.15	**0.74**	0.41 0.04	0.43	**0.72**	**0.76**
mTemp – P95	**-0.79**	-0.18	**0.60**	0.31 -0.13	0.37	**0.53**	**0.52**
mTemp – P99	**-0.79**	-0.30	**0.54**	0.24 -0.13	0.34	**0.43**	**0.37**
mTemp – diffM	**-0.75**	-0.43	0.04	0.13 -0.33	0.26	0.01	0.05
mTemp – diffE	**-0.67**	-0.34	0.11	-0.06 -0.13	0.18	0	**-0.38**
tGrad – STD	**0.45**	0.13	-0.01	-0.08 -0.12	-0.38	0.23	-0.27
tGrad – P50	**0.40**	0.10	-0.13	-0.08 -0.17	-0.42	-0.05	**-0.48**
tGrad – P95	**0.52**	0.21	-0.05	-0.07 -0.12	-0.38	0.17	**-0.35**
tGrad – P99	**0.45**	0.15	-0.16	-0.08 -0.12	-0.36	0.14	**-0.34**
tGrad – diffM	**0.44**	0.20	0.10	-0.05	-0.31	0.34	-0.08
tGrad – diffE	0.26	0	-0.28	-0.08 -0.07	-0.18	0	0.01
NAO – STD	**-0.42**	0.12	**0.34**	0.37 0.32	**0.44**	**0.70**	**0.58**
NAO – P50	-0.12 -0.12	0.67 **0.67**	**0.64**	0.54 0.55	0.52	**0.86**	**0.80**
NAO – P95	**-0.43**	0.28	**0.53**	**0.40**	**0.46**	**0.79**	**0.70**
NAO – P99	**-0.48**	-0.03	**0.50**	**0.39**	**0.43**	**0.70**	**0.57**
NAO – diffM	**-0.46**	-0.29	0.07	0.18	**0.36**	0.48	0.34
NAO – diffE	**-0.49**	**-0.50**	0.14	0.21	0.22	-0.06	-0.30